THE BLOOD SUPPLY AND VASCULAR DISORDERS OF THE HUMAN SPINAL CORD

VOLUME II FIGURES.

A Thesis submitted for the Degree of
Doctor of Philosophy in the University of Oxford
by

J. TREVOR HUGHES



Magdalen College,
Oxford.

Trinity Term, 1967.

Fig. 1.

The anterior spinal artery.

Willis (1667)

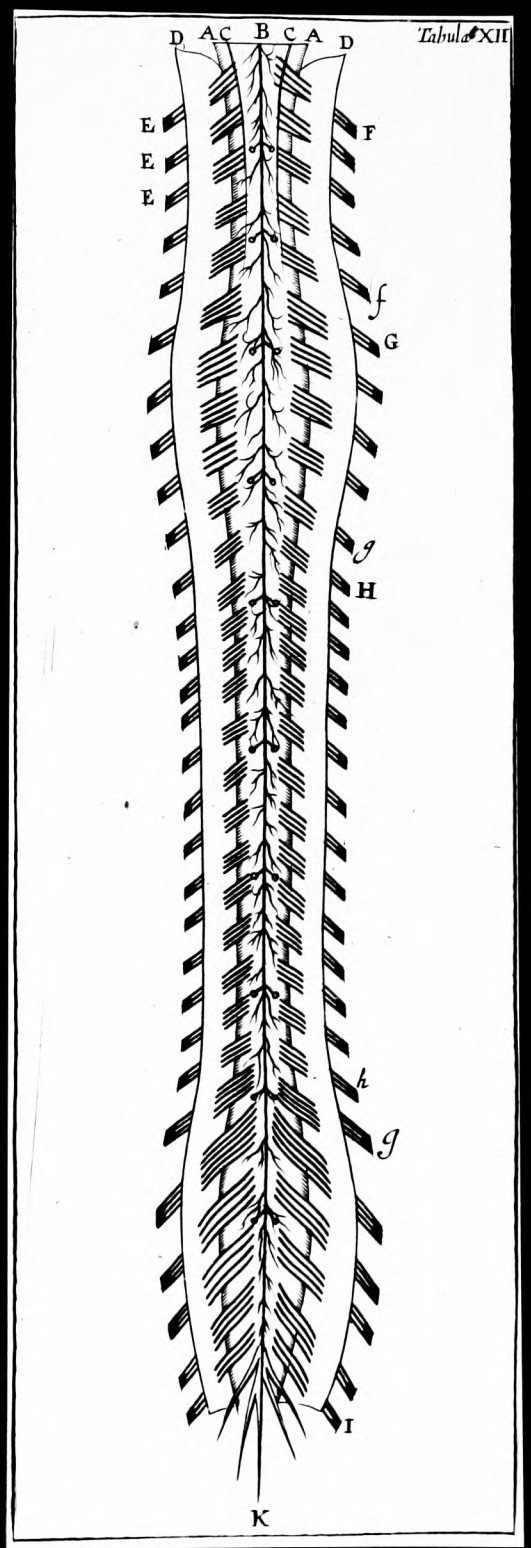

Tabula XII
D A C B C A D
E
E
E
F
f
G
g
H
h
g
I
K

Fig. 2.

The anterior spinal artery.

Willis (1667)

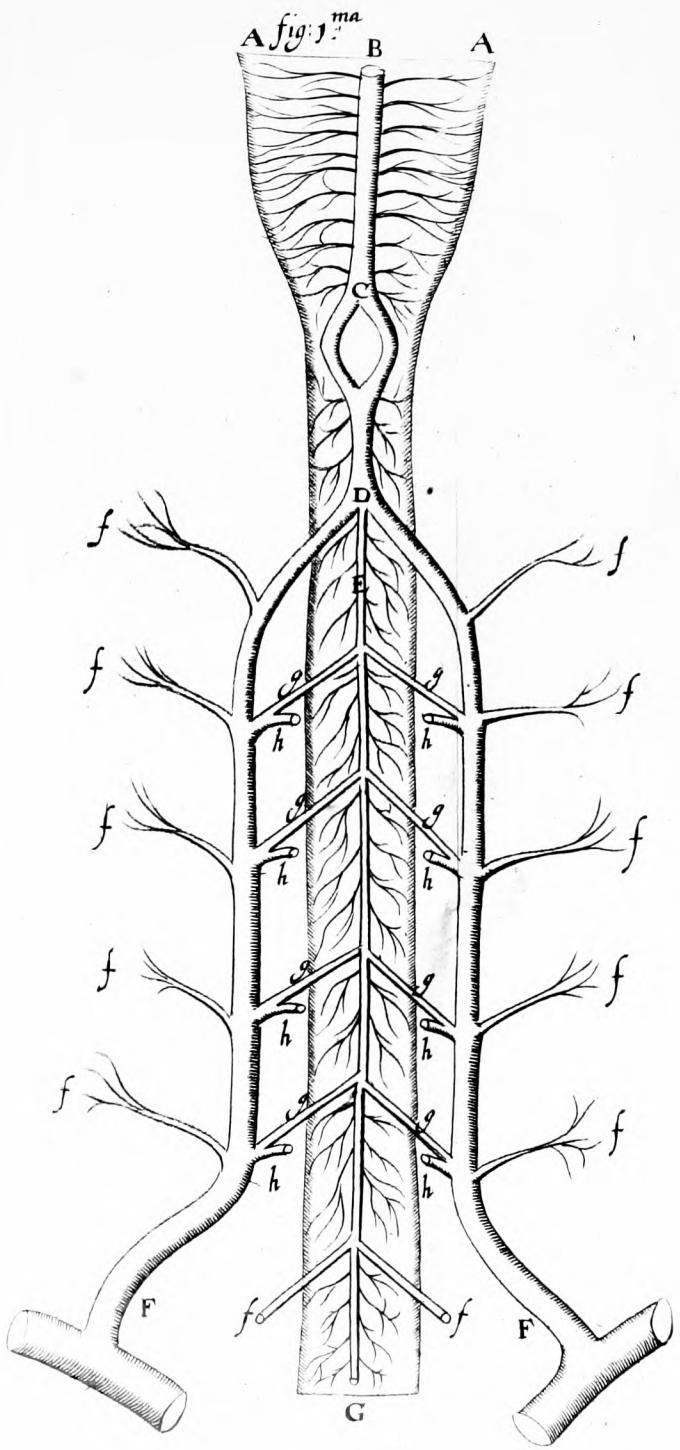


fig. 2da
A

Fig. 3.

The anterior and posterior spinal arteries.

Vieussens (1684)

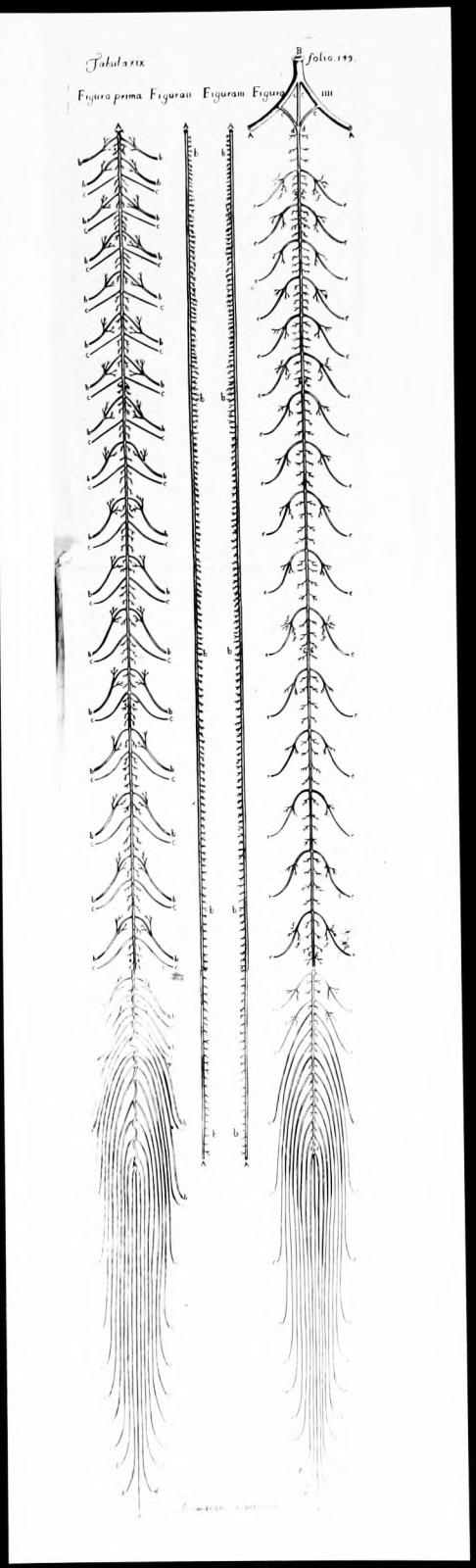

Tabula xix
folio 199
Figura prima
Figuram
Figuram
Figura
IIII

Fig. 4.

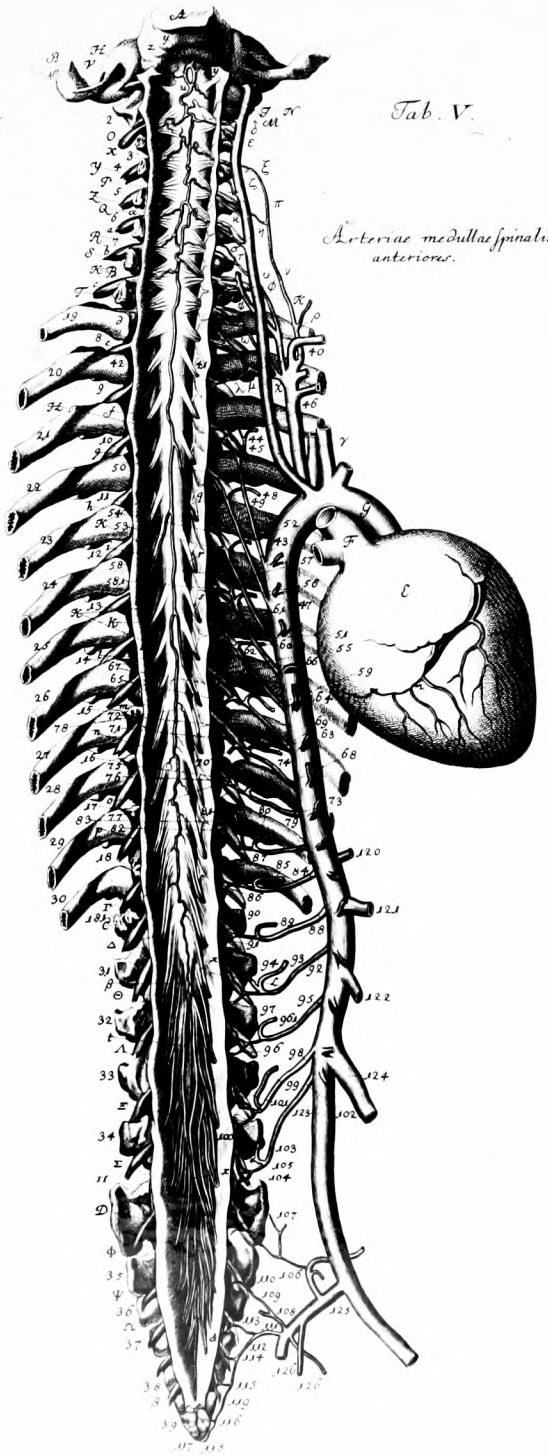
The anterior spinal artery.

Haller (1756)

Fasc. VII

Tab. V.

Arteriae medullares spinales anteriores.



Kaltenhofer del.

Ziegler sculps.

Fig. 5.

The posterior spinal artery.

Haller (1756)

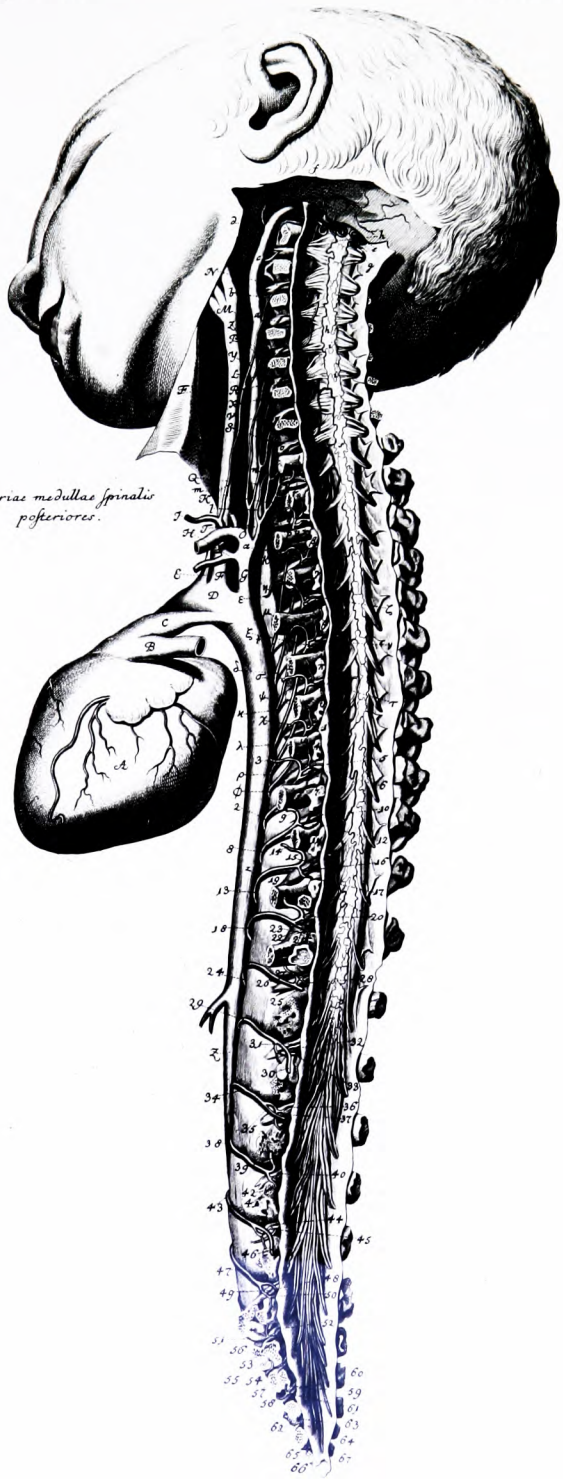

Arteriae medullae spinalis posteriores.

Fig. 6.

Diagram of the segmental vascular supply of the human spinal cord.

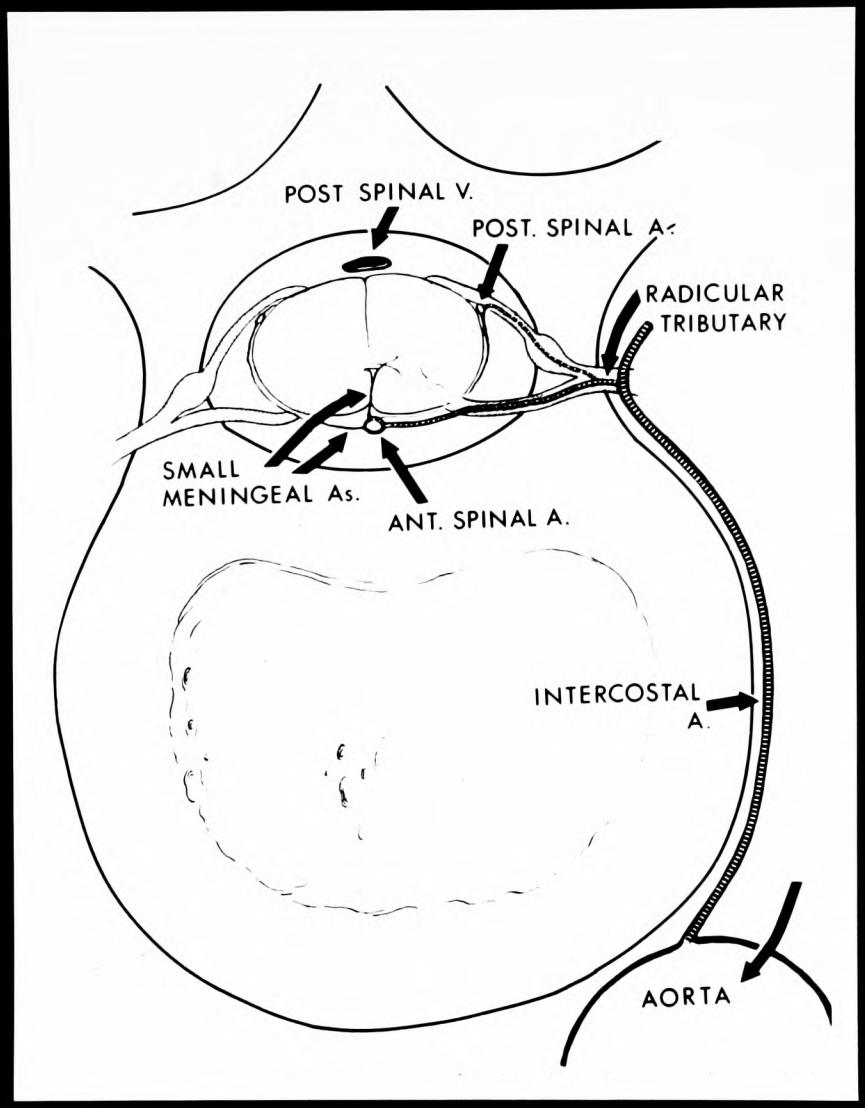

POST SPINAL V.
POST. SPINAL A.
RADICULAR TRIBUTARY
SMALL MENINGEAL As.
ANT. SPINAL A.
INTERCOSTAL A.
AORTA

Fig. 7.

Drawings of human spinal arteries injected with indian ink.

Left. Anterior spinal artery.

Right. Posterior spinal arteries.

ARTERIES

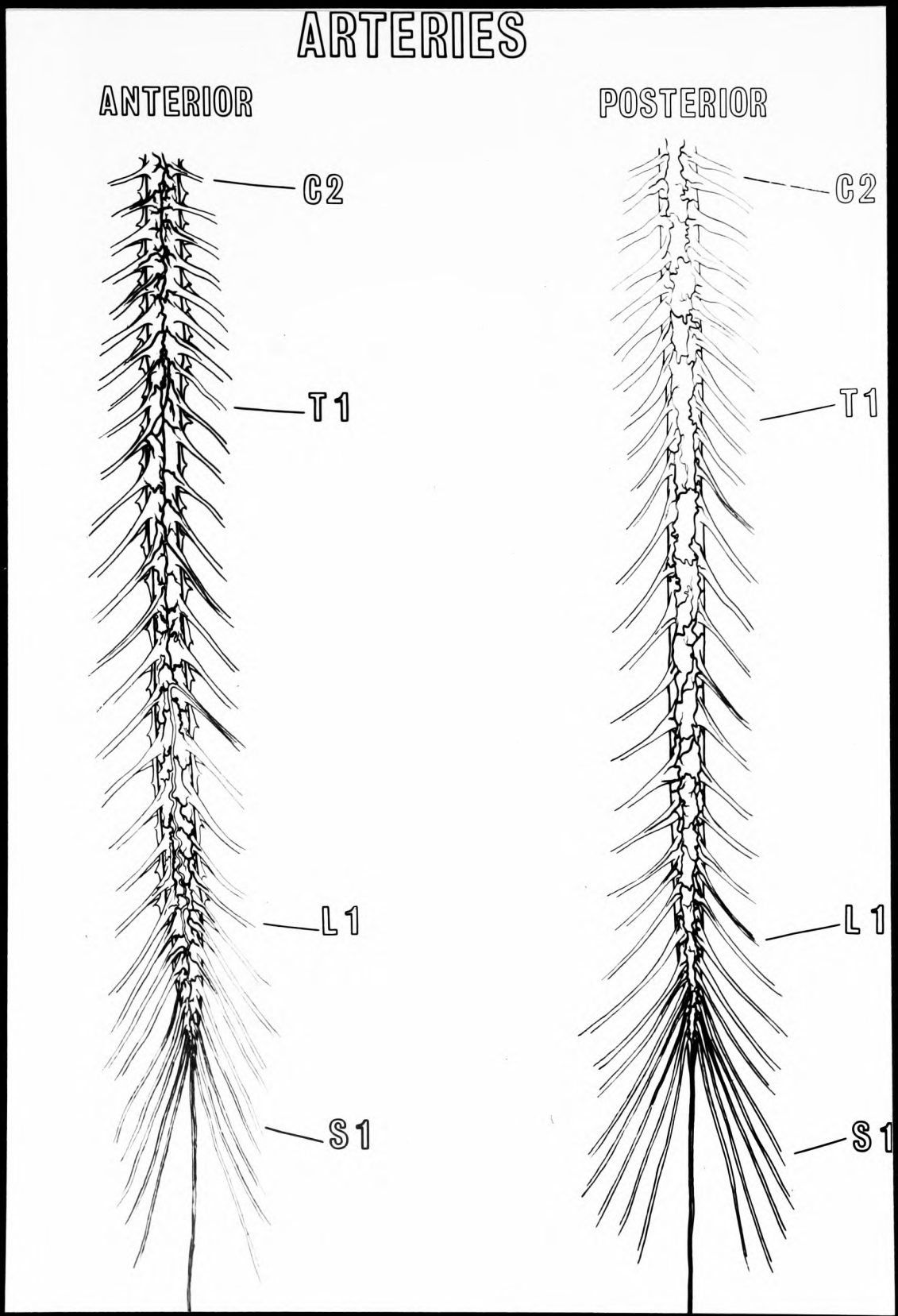
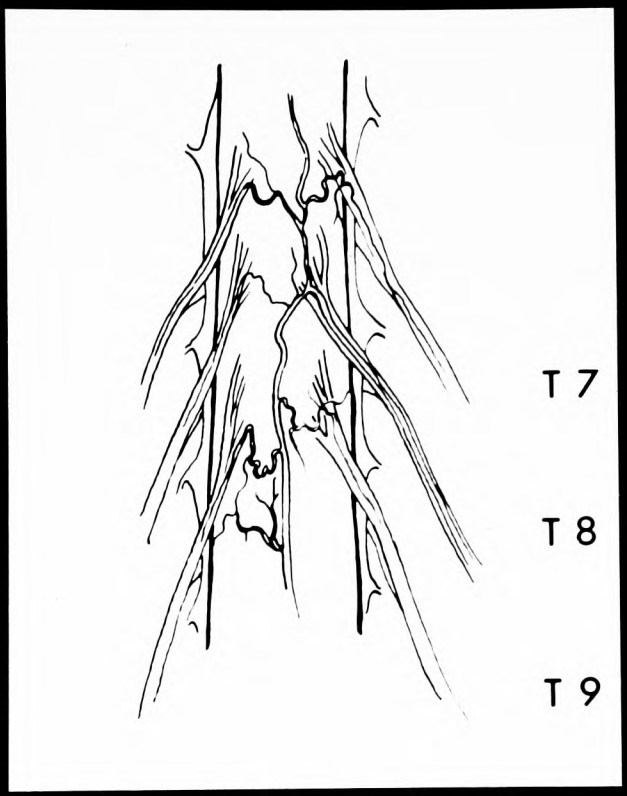
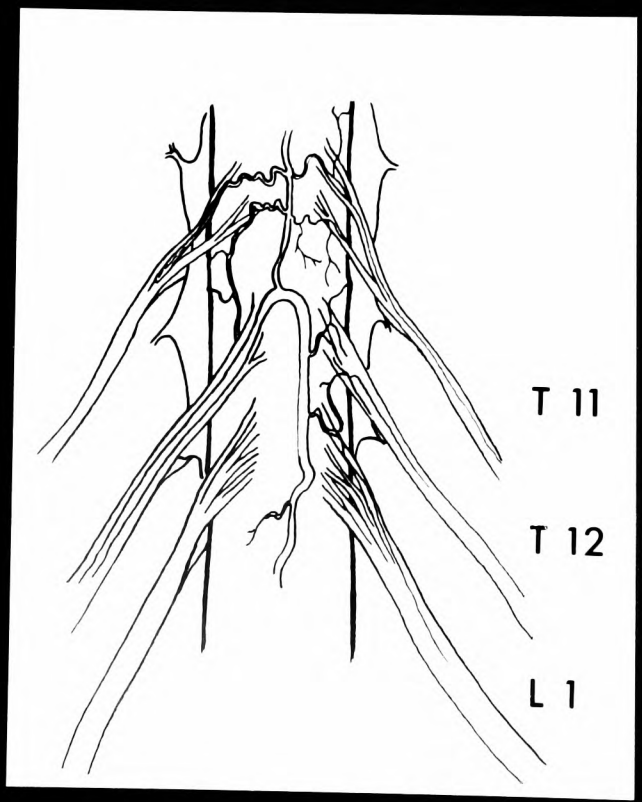


Fig. 8.

Drawings of radicular tributary arteries accompanying left T8 (fig 8a) and right T12 (fig 8b) anterior nerve roots.



8a



8b

Fig. 9.

Drawings of human spinal veins.

Left. Anterior veins.

Right. Posterior veins.

VEINS

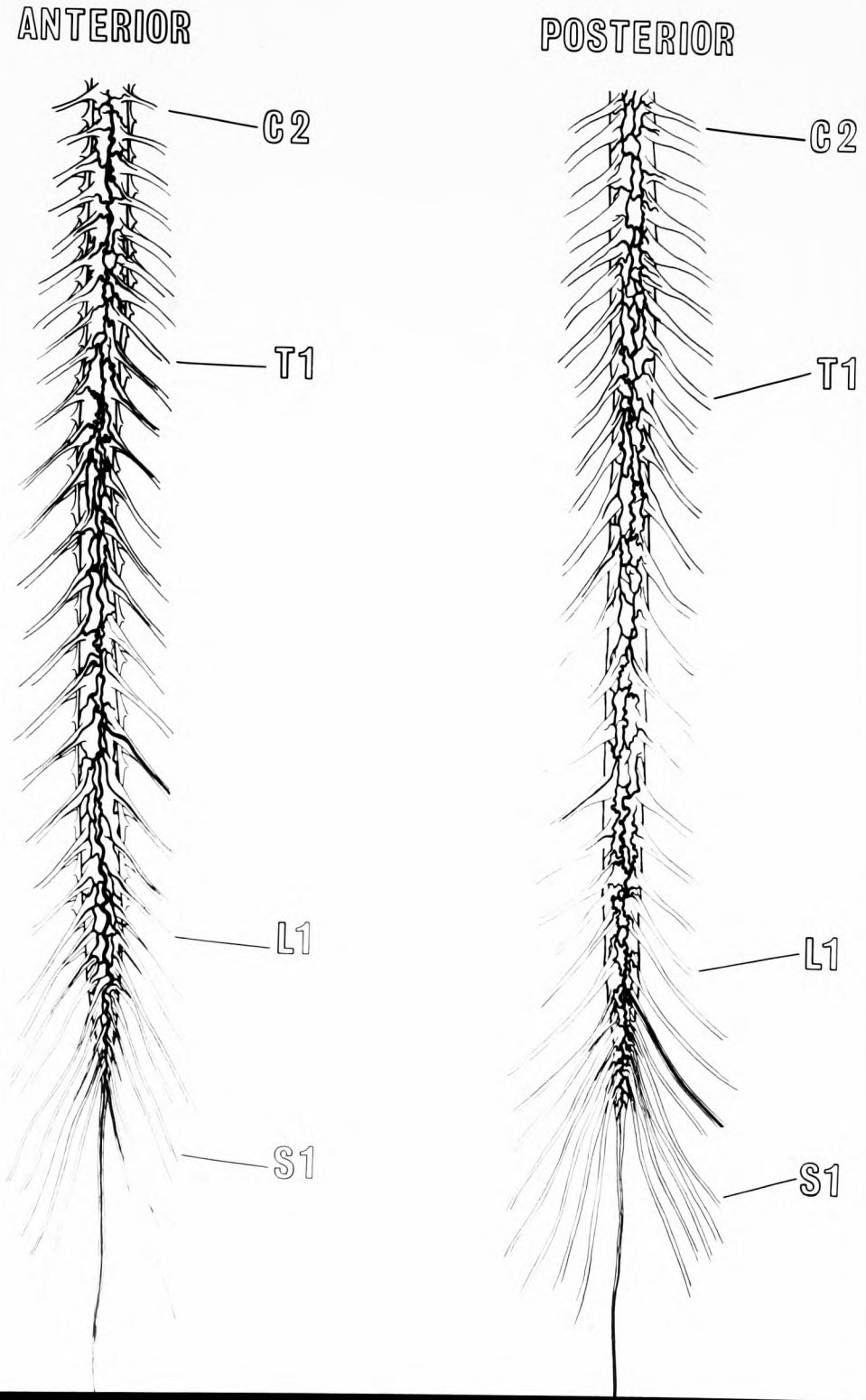


Fig. 10.

X-ray picture of human spinal arteries injected with barium sulphate suspension. The cervical and upper thoracic regions are shown. The anterior spinal artery (duplicated in the cervical region) receives two medium sized cervical tributaries and two larger thoracic tributaries.



10

Fig. 11.

Anterior aspect of human spinal cord.

The spinal arteries have been injected with indian ink which shows three major tributaries to the anterior spinal artery. The largest tributary (Artery of Adamkiewicz) accompanies the left T10 spinal nerve root.



11

Fig. 12.

Posterior aspect of human spinal cord.

The spinal arteries have been injected with indian ink introduced into the largest anterior radicular tributary. The posterior spinal arteries have filled *via* an anastomotic vessel around the conus medullaris.



12

Figs. 13, 14, 15.

Human spinal cord injected with barium sulphate suspension which distinguishes the white injected arteries from the veins. The pictures show the largest anterior tributary artery (fig 13), small anterior tributaries (fig 14) and the irregular posterior spinal arteries (fig 15).



13



14



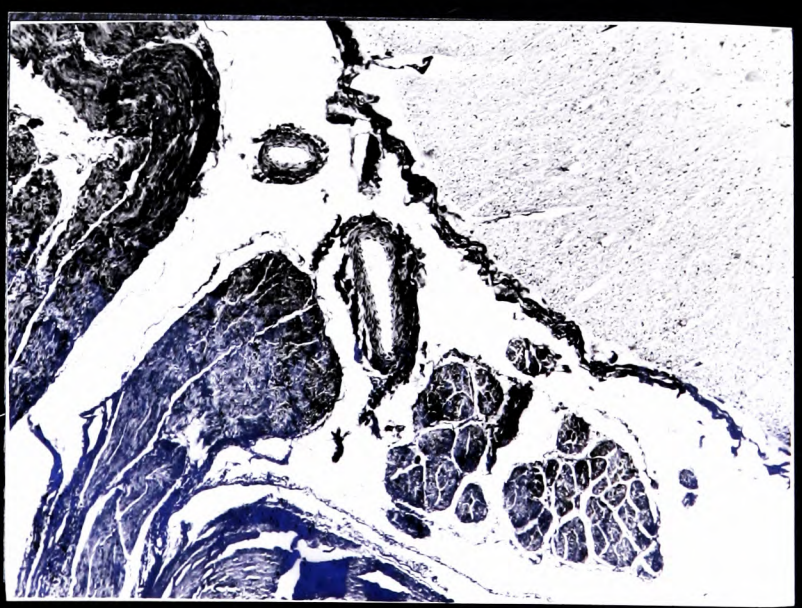
15

Fig. 16.

Transverse section of spinal cord with attached spinal nerve roots and posterior root ganglion. The major anterior tributary accompanying the anterior spinal nerve root (fig 16b) is seen to be of the same size as the anterior spinal artery (fig 16a).



16a



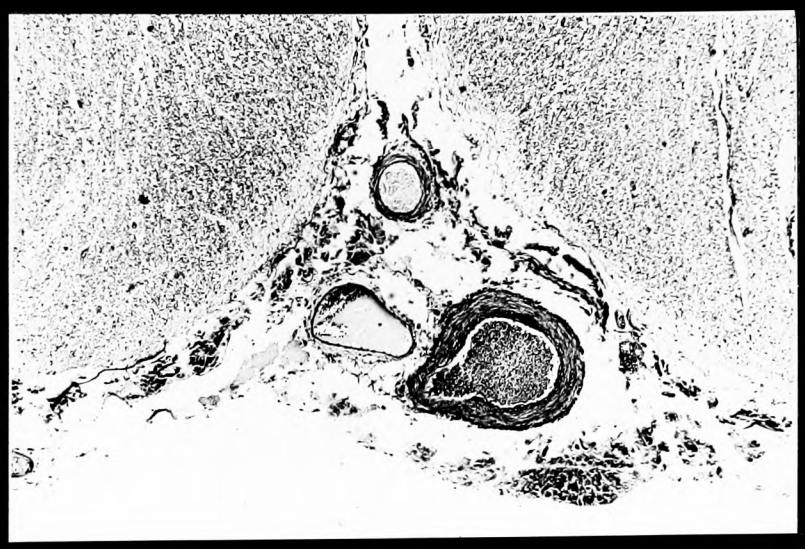
16b

Figs 17, 18.

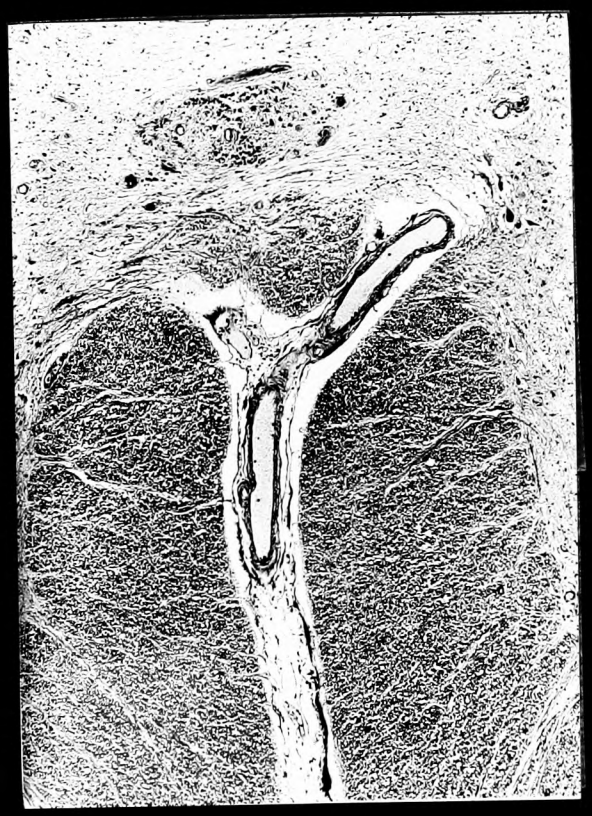
These photomicrographs are from a transverse section of a human spinal cord.

Fig. 17. Anterior spinal artery and vein. (Haematoxylin and Van Gieson X 55)

Fig. 18. Sulcal artery (Haematoxylin and Van Gieson X 55).



17



18

Fig. 19.

Human lumbar cord injected with barium sulphate suspension, cleared in oil of wintergreen and sliced transversely. When viewed by transmitted light the intramedullary vessels appear black. Note the course of the sulcal artery laterally into one grey column.



19

Figs. 20, 21, 22.

These photomicrographs are from a transverse section of a human spinal cord.

Fig. 20. Long penetrating vessel entering the spinal cord at the posterior root entry zone and supplying the posterior horn.
(Haematoxylin and Van Gieson X 50).

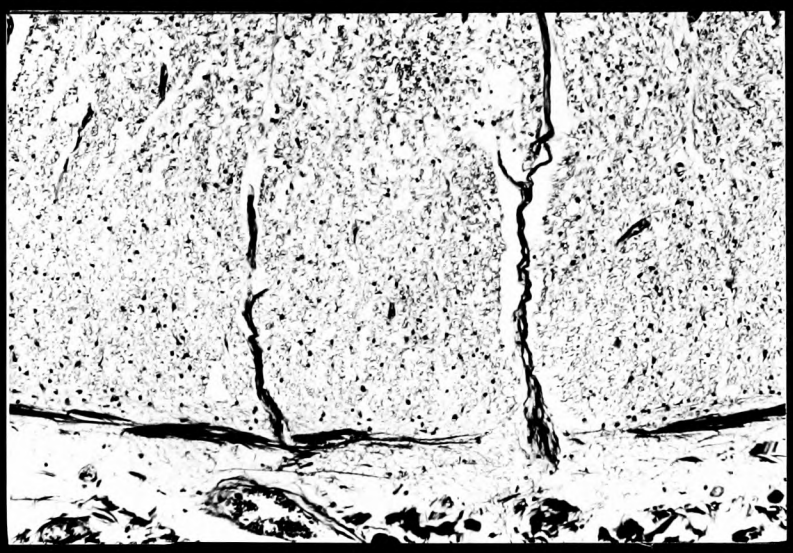
Fig. 21. Short radial vessels supplying peripheral rim of anterior white column.
(Haematoxylin and Van Gieson X 110).

Fig. 22. Posterior median spinal vein.
(Haematoxylin and Van Gieson X 50).

20



21



22



Figs 23, 24, 25.

These photomicrographs illustrate case 1 and are from transverse sections of the spinal cord stained for myelin. (Weil X 8).

Fig. 23. T3 segmental level. There is Wallerian degeneration evident in the posterior columns.

Fig. 24. T6 segmental level. There are large spongy areas of diffuse degeneration affecting the white matter.

Fig. 25. T7 segmental level. There are similar changes to those seen in T6.

23



24



25



Figs. 26, 27, 28.

These photomicrographs illustrate case 1 and are from transverse sections of the spinal cord stained for myelin (Weil X 8).

Fig. 26. T8 segmental level. There are large spongy areas of degeneration affecting the white matter.

Fig. 27. T10 segmental level. There is diffuse degeneration of the white matter combined with Wallerian degeneration of long tracts.

Fig. 28. L1 segmental level. The appearances are similar to fig 27.

26



27



28



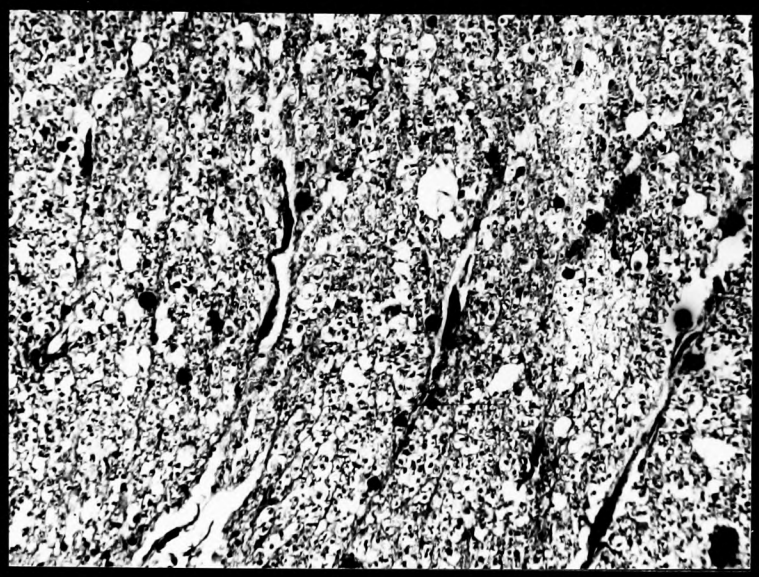
Figs. 29, 30, 31.

These photomicrographs illustrate case 1 and are from transverse sections of the spinal cord.

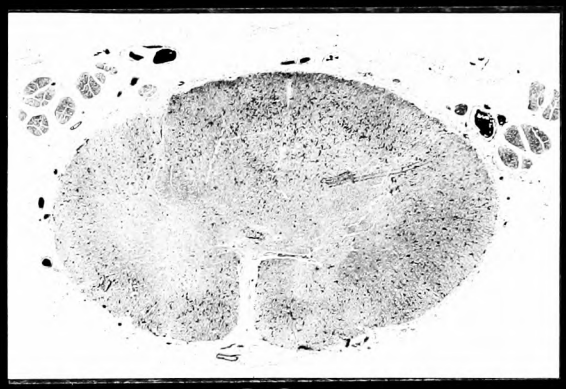
Fig. 29. T8 segmental level, to show large spongy areas of diffuse degeneration in one anterior column.
(Haematoxylin and eosin X 90).

Fig. 30. T10 segmental level. Large numbers of corpora amylacea are present throughout the spinal cord.
(Haematoxylin and eosin X 8).

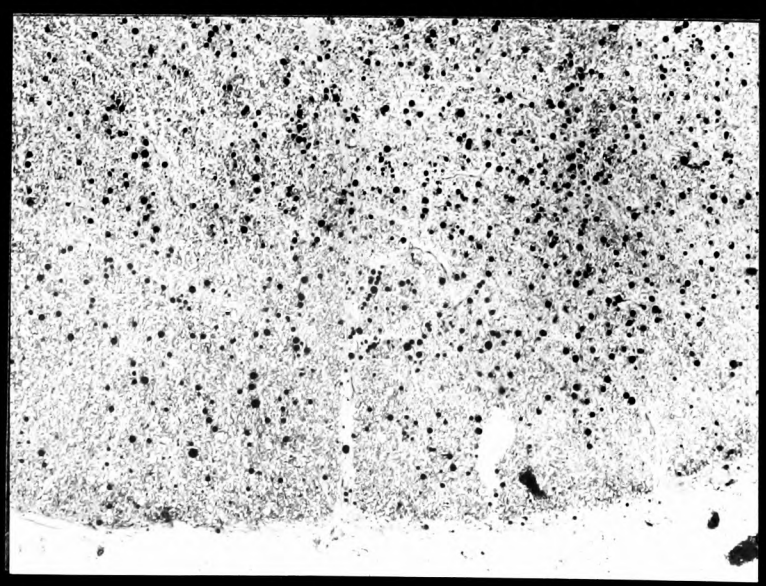
Fig. 31. High power view of the same section seen in fig 30.
(Haematoxylin and eosin X 85).



29



30



31

Figs. 32, 33, 34.

These photomicrographs illustrate case 1 and are from transverse sections of the spinal cord.

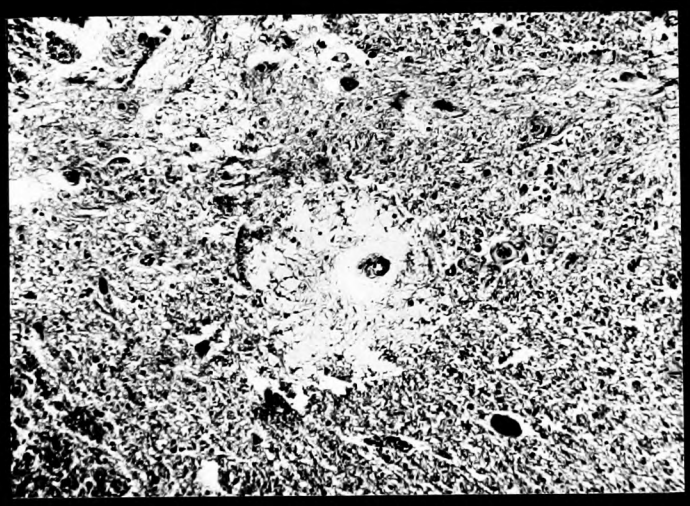
Fig. 32. T8 segmental level. Small focal area of necrosis in one lateral column. (Weil X70).

Fig. 33. T4 segmental level. Small focal area of necrosis in one anterior horn. (Haematoxylin and Van Gieson X 70).

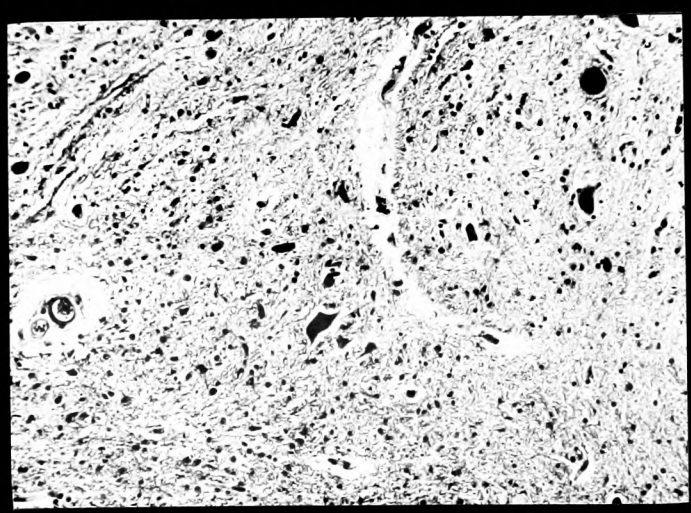
Fig. 34. L1 segmental level. Neurone cell bodies in anterior horn. (Haematoxylin and eosin X 70).



32



33



34

Figs. 35, 36, 37.

These photomicrographs illustrate case 2 and are from transverse sections of the spinal cord stained for myelin (Weil X 8).

Fig. 35. C7 segmental level. Wallerian degeneration is present in the posterior columns.

Fig. 36. T4 segmental level. There is Wallerian degeneration in the posterior columns and diffuse degeneration of the white matter.

Fig. 37. L1 segmental level. There is diffuse degeneration combined with Wallerian degeneration of long tracts.



35



36



37

Fig. 38.

Abdominal aorta of case 3. The aorta has been opened and is viewed from its anterior aspect. Severe ulcerating and calcifying atheroma affects the lower abdominal aorta which contains antemortem thrombus on the posterior wall, at the bifurcation, and passing into the left common iliac artery. Note the relationship of the thrombus to the lumbar arteries. The ostia of the fourth lumbar arteries are concealed behind thrombus. (Half natural size).



38

Fig. 39.

Abdominal aorta of case 4. The aorta has been opened and is viewed from its anterior aspect. There is severe ulcerating and calcifying atheroma with a large fusiform atherosclerotic aneurysm affecting the lower abdominal aorta. The aneurysm is filled with antemortem thrombus which conceals the orifices of the lumbar arteries. (Half natural size).

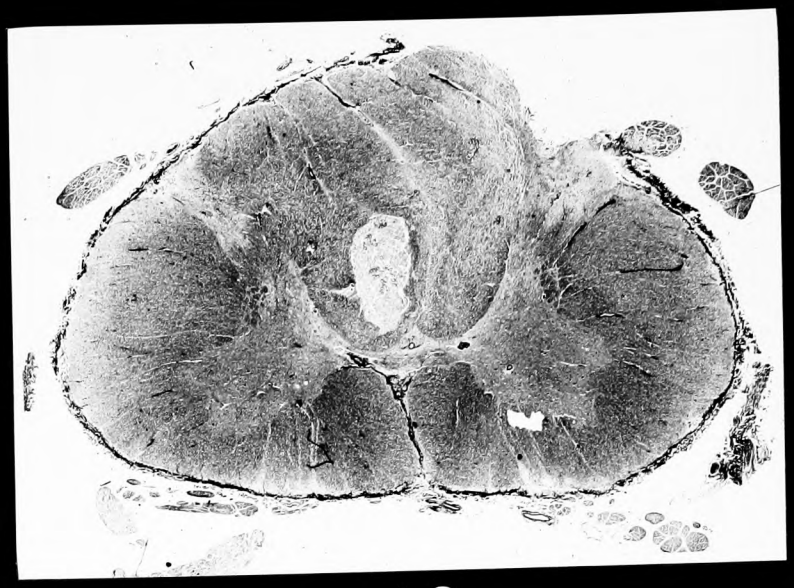


Figs. 40, 41.

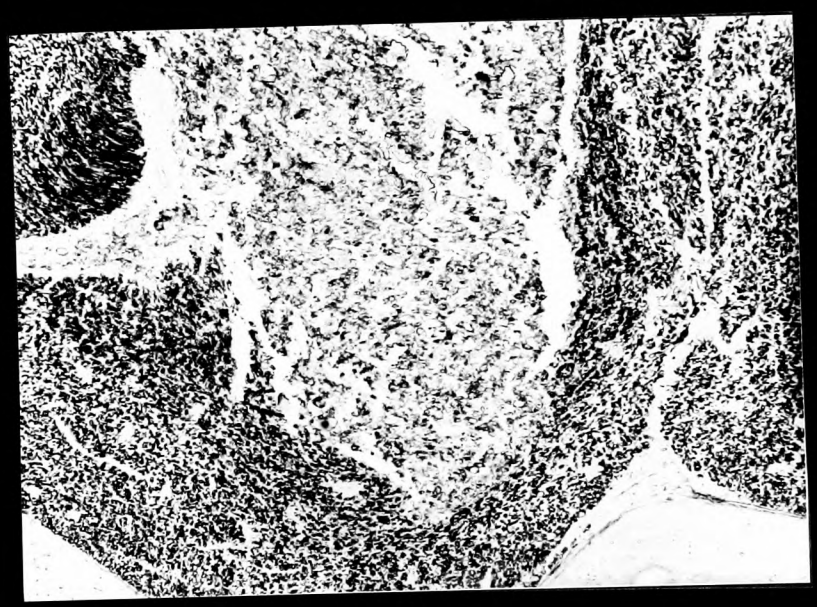
These photomicrographs illustrate case 4.

Fig. 40. Transverse section of spinal cord at C7 segmental level. There is an oval area of infarction in the posterior columns. (Weil X 7).

Fig. 41. Photomicrograph at higher magnification of the posterior columns at C7 segmental level. The myelin tubes are swollen and fragmented. (Weil X 50).



40



41

Figs. 42, 43.

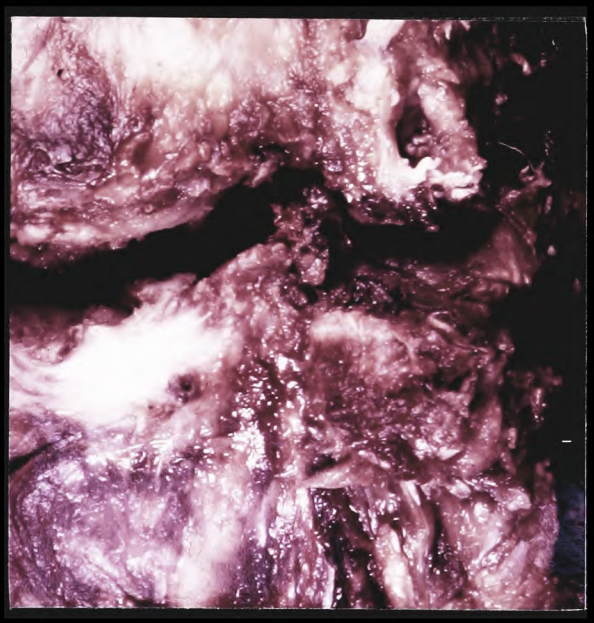
These photographs illustrate case 6.

Fig. 42. Anterior aspect of cervical spine as seen at necropsy. The C5-6 intervertebral disc is torn. (Approximately life size).

Fig. 43. Detail of fig. 42 showing left vertebral artery embedded in blood clot. (X 1½).



42



43

Figs. 44, 45.

These photographs are of the spinal cord in case 6. Approximately twice natural size.

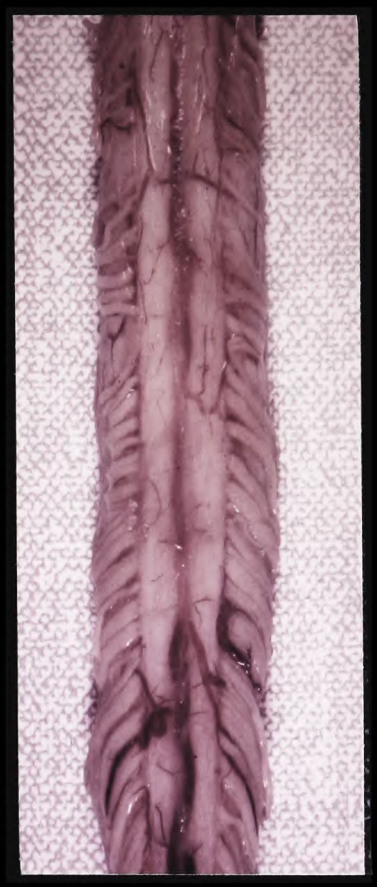
Fig. 44. Anterior aspect.

Fig. 45. Posterior aspect.

There is slight swelling affecting C5, 6 and 7 spinal-cord segments.



44



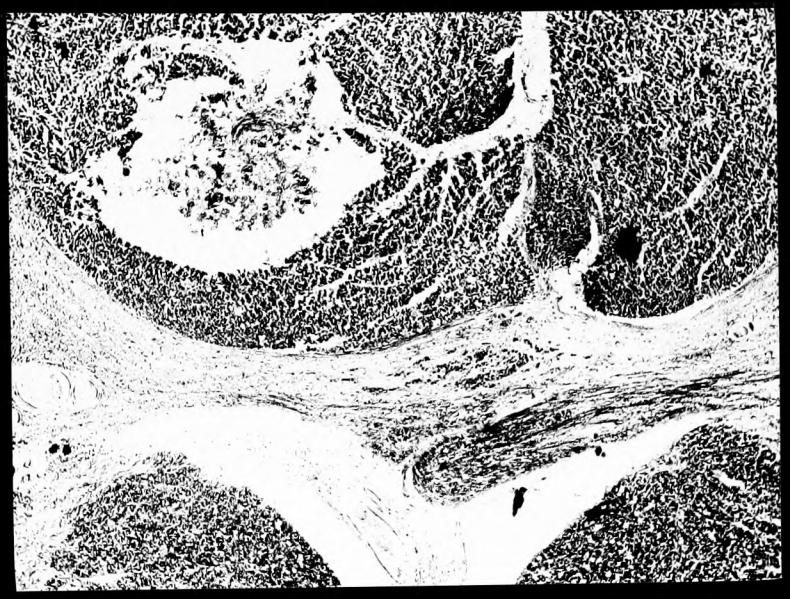
45

Figs. 46, 47.

These photomicrographs illustrate case 6.

Fig. 46. Transverse section at C4 segmental level showing the cephalic limit of the infarcted "cone" as a round area of necrosis in the right posterior column. (Weil X 30).

Fig. 47. Transverse section at C6 segmental level showing infarction involving most of the grey matter and some of the adjacent white matter. (Weil X 8).



46



47

Figs. 48, 49.

These photographs are of case 7.

Fig. 48. Medial aspect of right half of cervical spine sawn sagittally and showing normal vertebral bodies and spinal canal. There is a complete tear through the C5-6 intervertebral disc. (Approximately life size).

Fig. 49. Anterior aspect of cervical spine showing tear through the C5-6 intervertebral disc. (Slightly larger than life size).



48



49

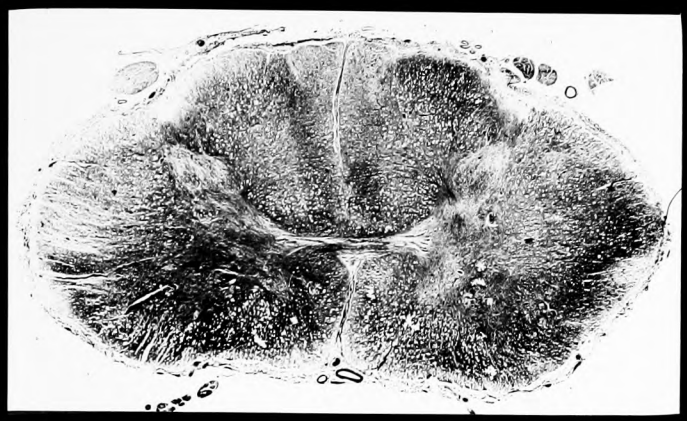
Figs. 50, 51, 52.

These photomicrographs illustrate case 7.

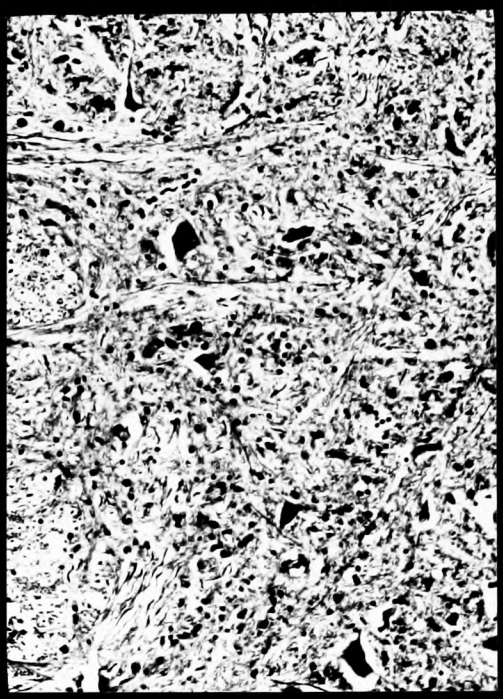
Fig. 50. Transverse section of spinal cord at C7 segmental level. There is a generalised loss of myelin and nerve fibres (fig. 52) with gliosis. (Weil X 6).

Fig. 51. Anterior horn at C8 segmental level showing shrunken pyknotic neurone cell bodies. (Haematoxylin and eosin X 125).

Fig. 52. Anterior median sulcus, grey commissure, anterior horn and anterior white column at C7 segmental level. The white matter is spongy due to loss of myelin (fig 50) and nerve fibres. (Holmes X 40).



50



51



52

Figs. 53, 54, 55.

These photographs (approximately twice natural size) are of the anterior aspect of the spinal cord in case 8.

Fig. 53. Thoracic region showing atrophy and greyish discoloration.

Fig. 54. View to show the cut surface with atrophy and discoloration of the anterior part of the spinal cord.

Fig. 55. Normal lumbar and sacral regions with a major radicular tributary accompanying left L2 spinal nerve root.



53



54



55

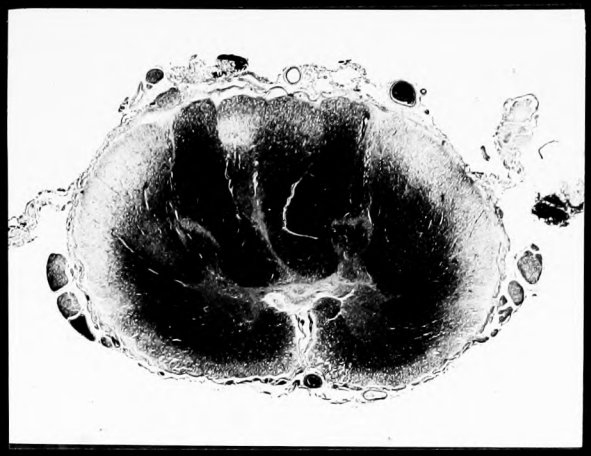
Figs. 56, 57, 58, 59.

These photomicrographs illustrate case 8.

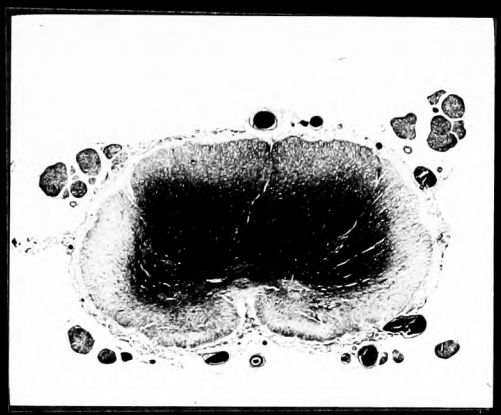
Fig. 56. T3.
Fig. 57. T10.
Fig. 58. L4.

Myelin stained transverse sections of the spinal cord. In T10 there is atrophy of the anterior two-thirds of the spinal cord. Wallerian degeneration is seen at T3 and L4. (Weil X 7·5).

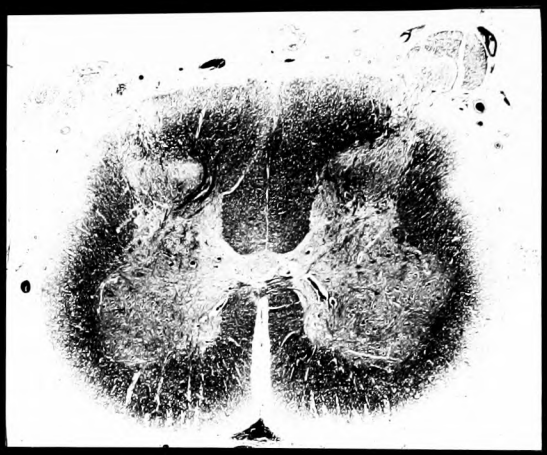
Fig. 59. Transverse section of spinal cord at T10 segmental level. The atrophied grey column and anterior white column on one side is illustrated. (Haematoxylin and Van Gieson X 37).



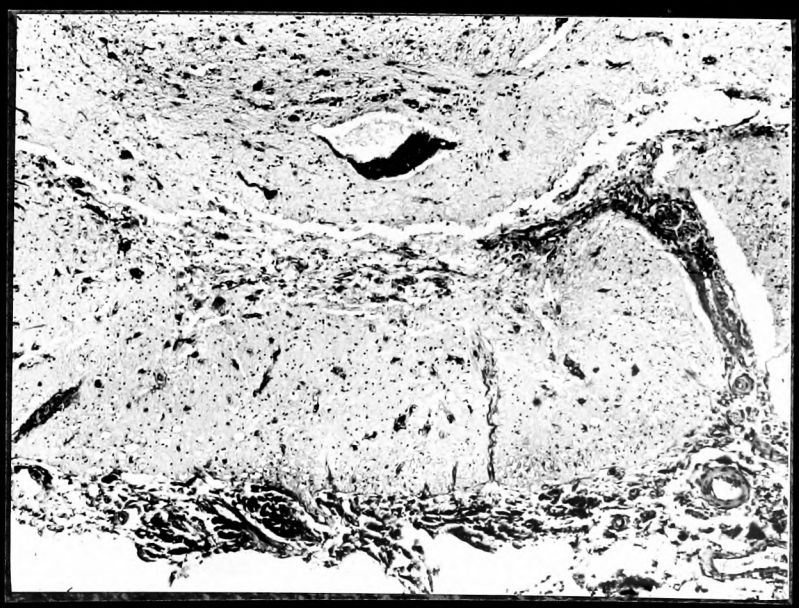
56



57



58



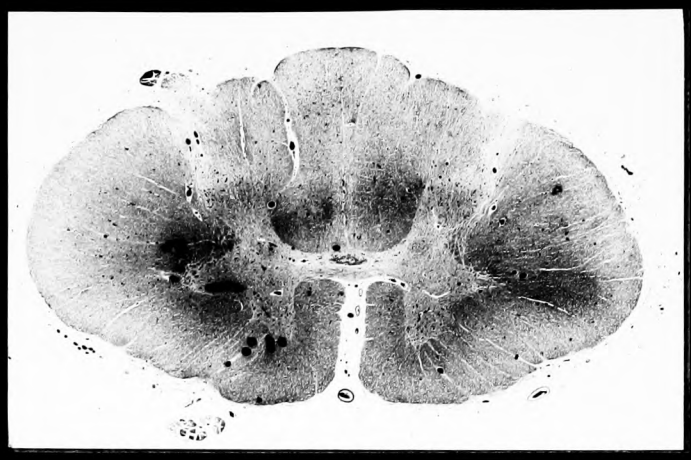
59

Figs. 60, 61.

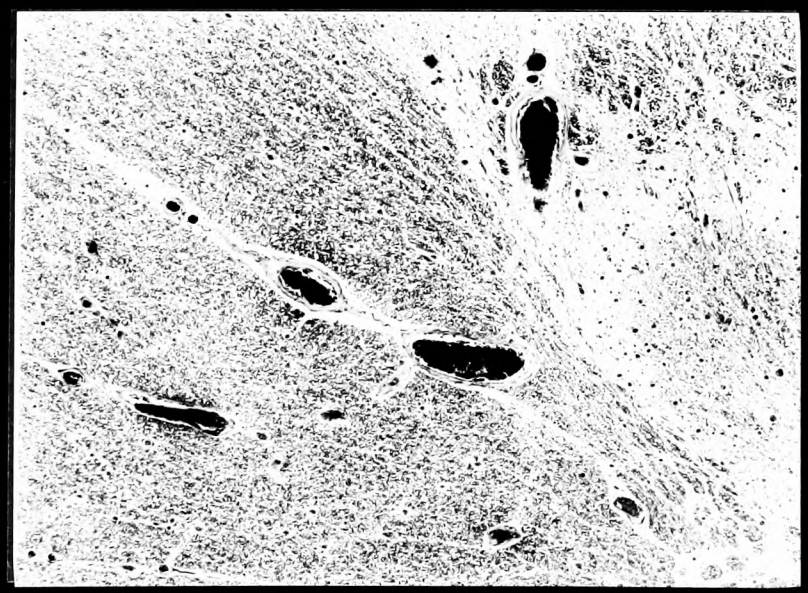
These photomicrographs illustrate case 9.

Fig. 60. Transverse section of spinal cord at T1 segmental level showing acute infarction with congestion and large distended vessels. (Haematoxylin and eosin X 8).

Fig. 61. Detail of congestion and distended veins around right posterior horn at C8 segmental level. (Haematoxylin and Van Gieson X 50).



60



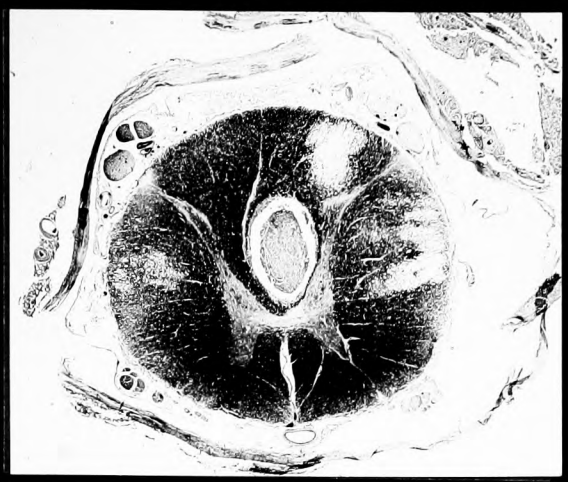
61

Figs. 62, 63, 64.

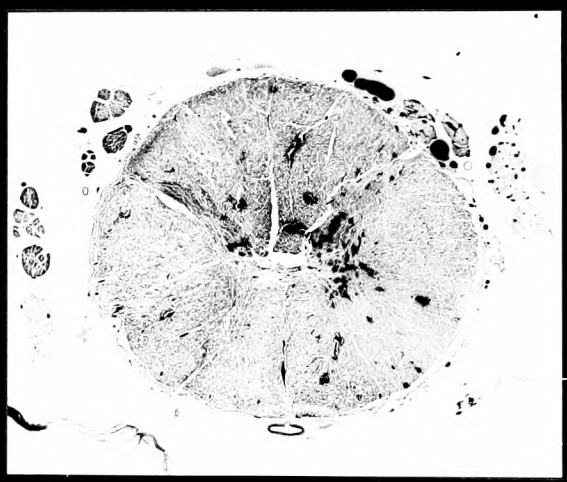
These photomicrographs illustrate case 10.

Fig. 62. T10.
Fig. 63. T12.
Fig. 64. L1.

Myelin stained transverse sections of spinal cord showing infarction extending from T10 to L1 and maximal at T12 segmental level. The infarct has the form of a spindle ending above (fig 62) and below (fig 64) in the posterior columns.



62



63



64

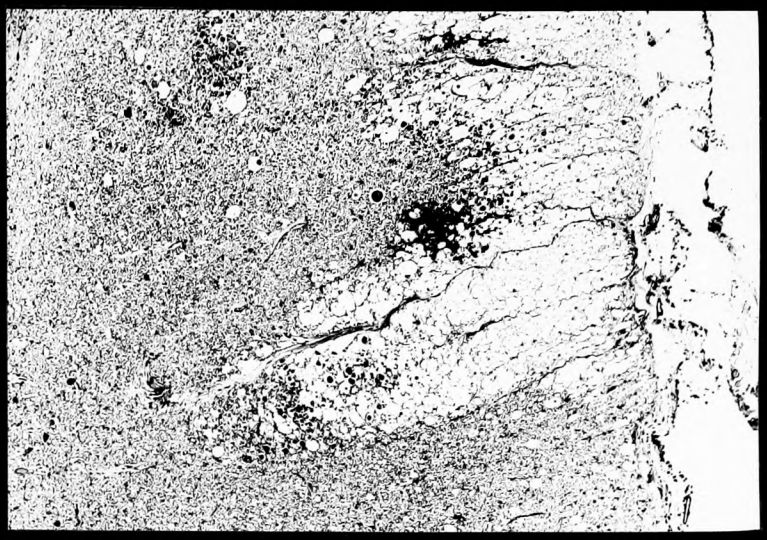
Figs. 65, 66, 67.

These photomicrographs illustrate case 10. They are all from transverse sections of the spinal cord (Haematoxylin and eosin X 37).

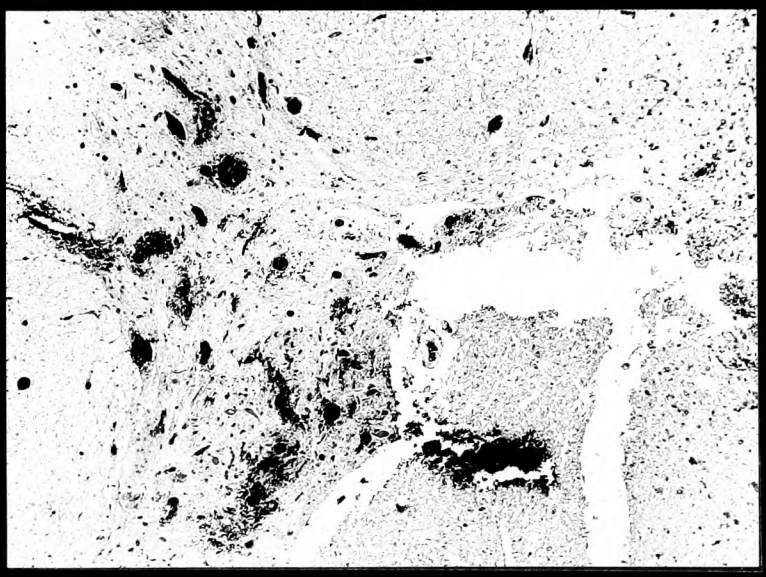
Fig. 65. T10. The detail of the infarction in the left lateral white column is shown. (See fig. 62).

Fig. 66. T12. The detail of the infarction in the left grey column is shown. (see fig. 63).

Fig. 67. T8. This illustration shows infiltrating tumour in the extradural space.



65



66



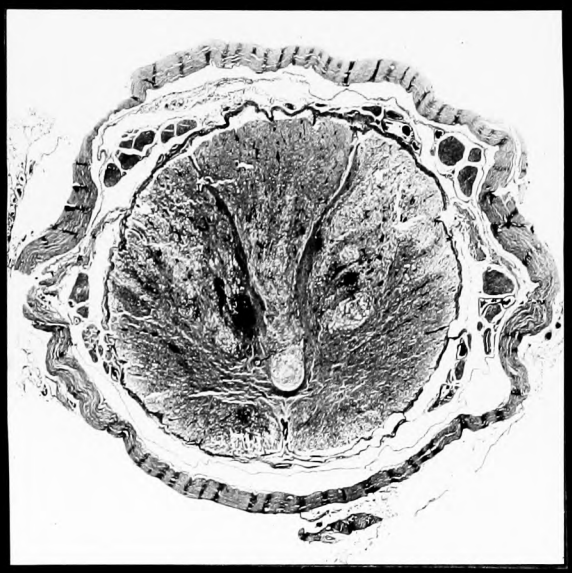
67

Figs. 68, 69.

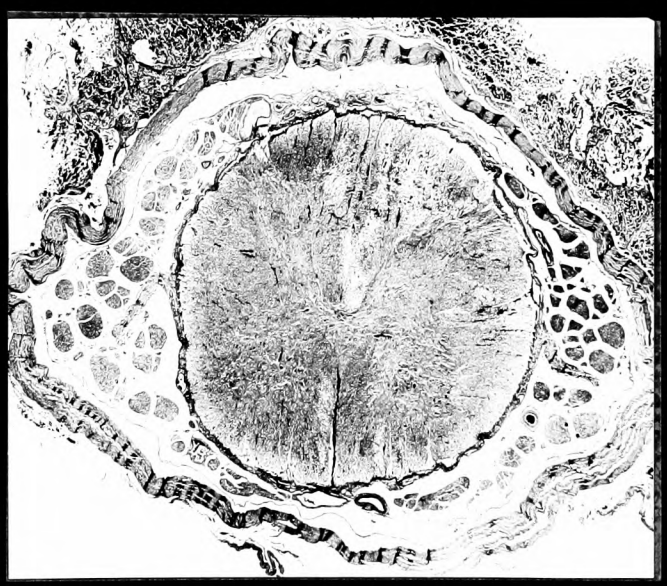
These photomicrographs illustrate case 11. They are both from transverse sections of the spinal cord stained for myelin (Weil X 7·5).

Fig. 68. T8 segmental level showing almost complete haemorrhagic infarction of the spinal cord.

Fig. 69. L3 segmental level showing partial infarction. There is extradural tumour but there was no compression of the spinal cord and no intradural tumour infiltration.



68



69

Figs. 70, 71, 72, 73.

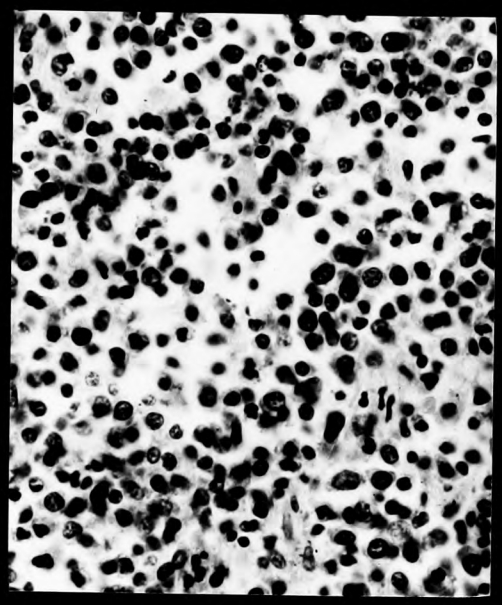
These photomicrographs illustrate case 12.

Fig. 70. Detail of tumour in lymph nodes. (Haematoxylin and eosin X 300).

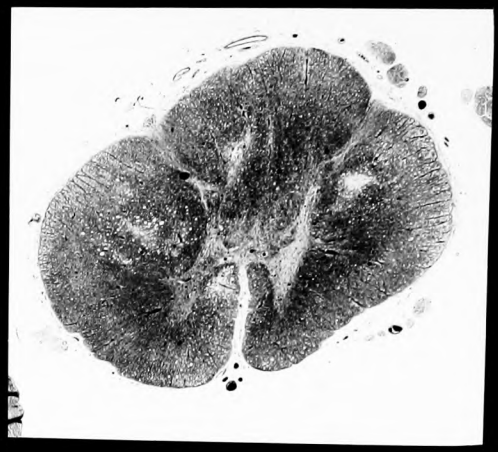
Fig. 71. Transverse sections at T6 segmental level showing spongy degeneration of white matter. (Weil X 6).

Fig. 72. Detail of left anterior horn, left anterior white column and anterior median sulcus at T6 segmental level. The grey matter is affected by ischaemic changes. (Haematoxylin and eosin X 40).

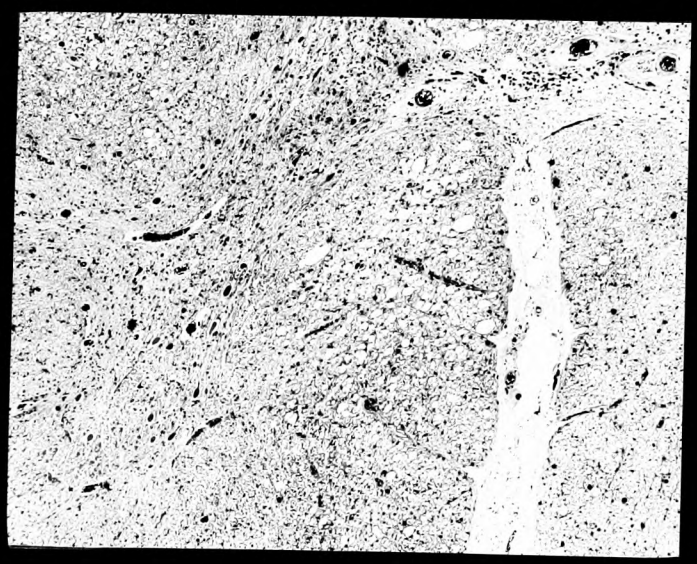
Fig. 73. Detail of right posterior column with infarction in territories of long penetrating vessels. (Haematoxylin and eosin X 105).



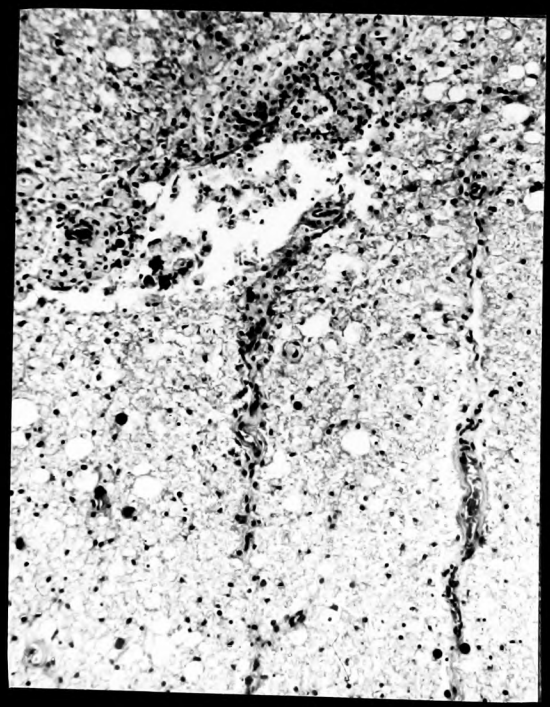
70



71



72



73

Figs. 74, 75, 76.

These photomicrographs illustrate case 13.

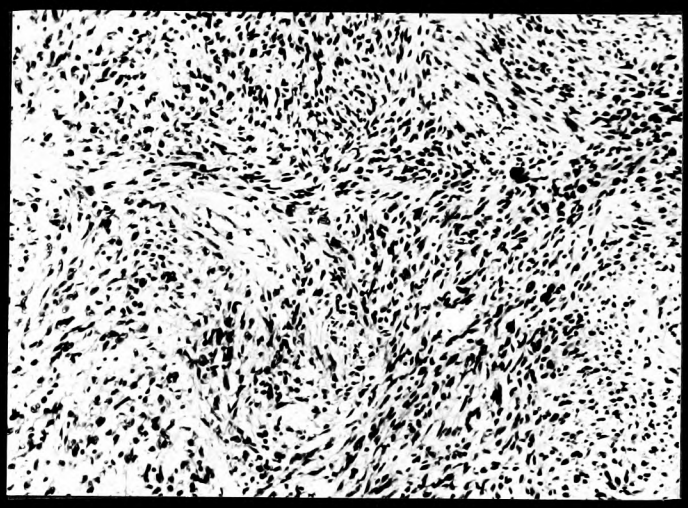
Fig. 74. Decalcified section cut through thoracic spine in region of intervertebral foramen which is completely occluded by tumour. (Haematoxylin and eosin X 120).

Fig. 75. Detail of fibrosarcoma seen in fig. 74. (Haematoxylin and eosin X 250).

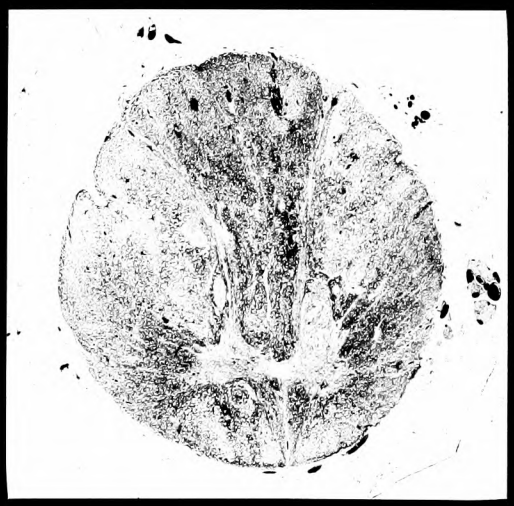
Fig. 76. Transverse section of spinal cord at T6 segmental level. There is infarction affecting most of the cross-sectional area and involving both grey and white matter. (Weil X 6·5).



74



75



76

Figs. 74, 75, 76.

These photomicrographs illustrate case 13.

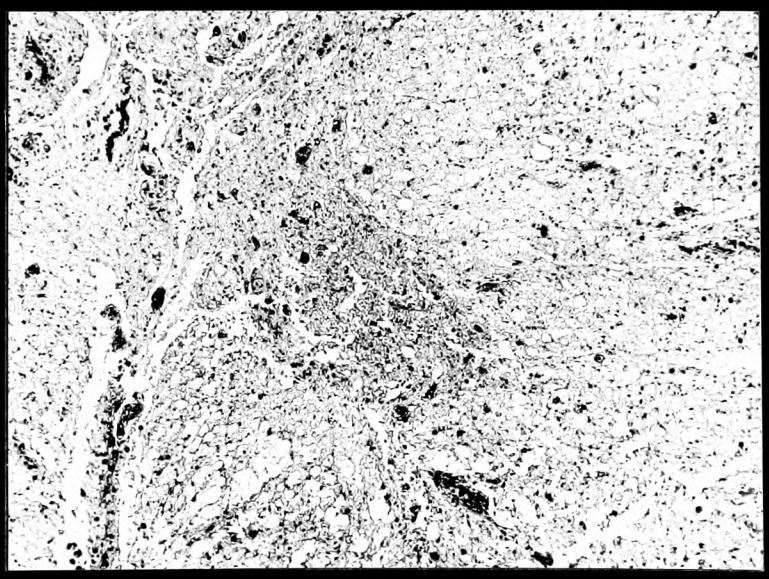
Fig. 74. Decalcified section cut through thoracic spine in region of intervertebral foramen which is completely occluded by tumour. (Haematoxylin and eosin X 120).

Fig. 75. Detail of fibrosarcoma seen in fig. 74. (Haematoxylin and eosin X 250).

Fig. 76. Transverse section of spinal cord at T6 segmental level. There is infarction affecting most of the cross-sectional area and involving both grey and white matter. (Weil X 6·5).



77



78

Figs. 79, 80, 81, 82.

These photomicrographs and photographs illustrate case 14.

Fig. 79. Decalcified section of thoracic spine in the region of the intervertebral foramen which is completely filled by infiltrating tumour. (Haematoxylin and eosin X 98).

Fig. 80. Anterior aspect of the spinal cord in the lower cervical and upper thoracic regions. The anterior spinal artery is flattened by slight pressure caused by kyphosis of the spine. (Approximately twice life size).

Fig. 81. Transverse section of the spinal cord at T3 segmental level showing marked ischaemic degeneration of the grey and white matter. (Weil X 6·5).

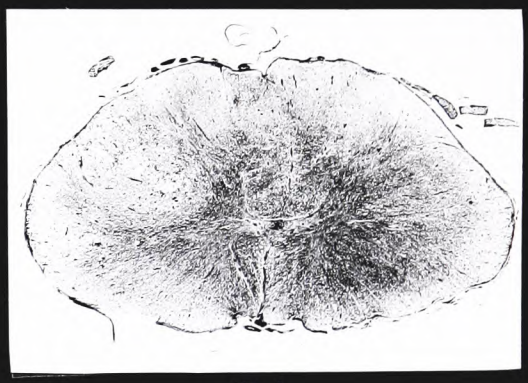
Fig. 82. Detail of spongy ischaemic degeneration affecting the left lateral white column. (Weil X 35).



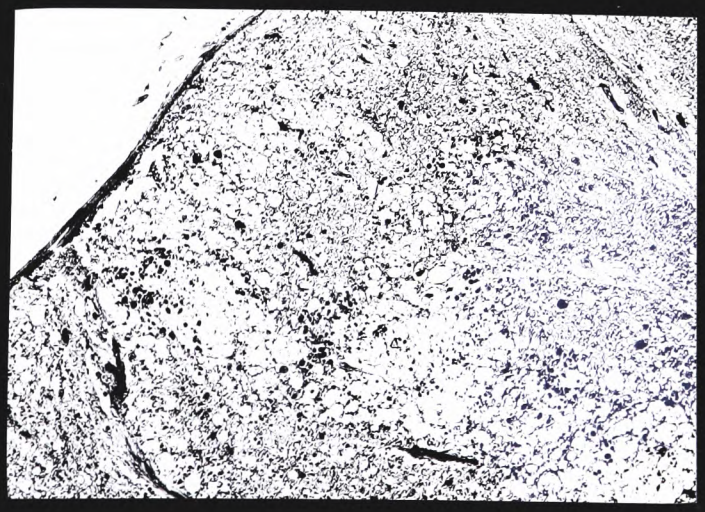
79



80



81



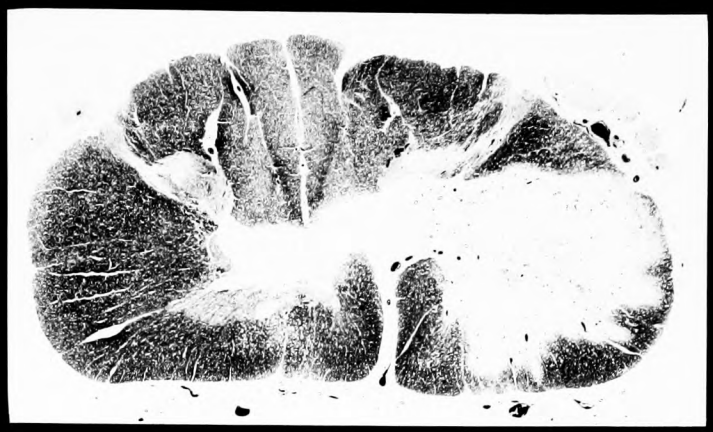
82

Figs. 83, 84, 85.

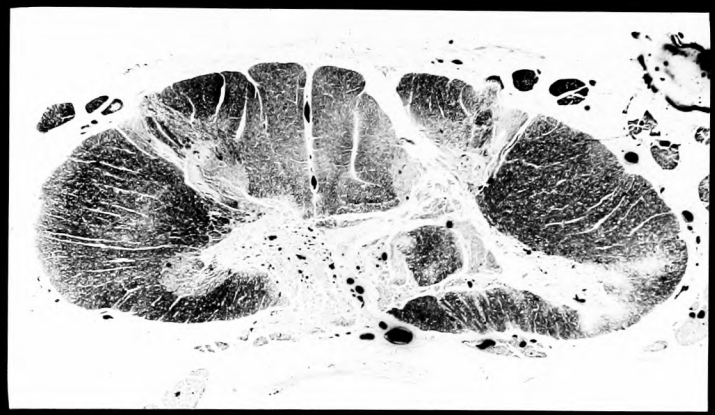
These photomicrographs illustrate case 15. All are transverse sections of the spinal cord stained for myelin. (Weil X 6·5).

Fig. 83. C3.
Fig. 84. C4.
Fig. 85. C5.

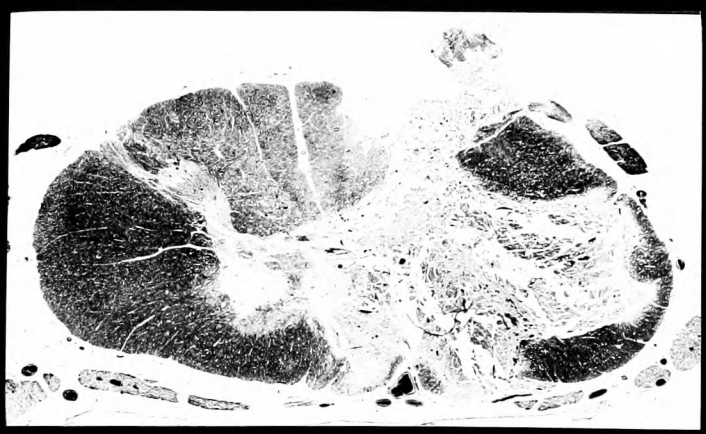
A large area of infarction affects the grey commissure, the anterior horns and parts of the white columns. The extension of the infarct into the anterior or lateral white columns is irregular and asymmetrical.



83



84



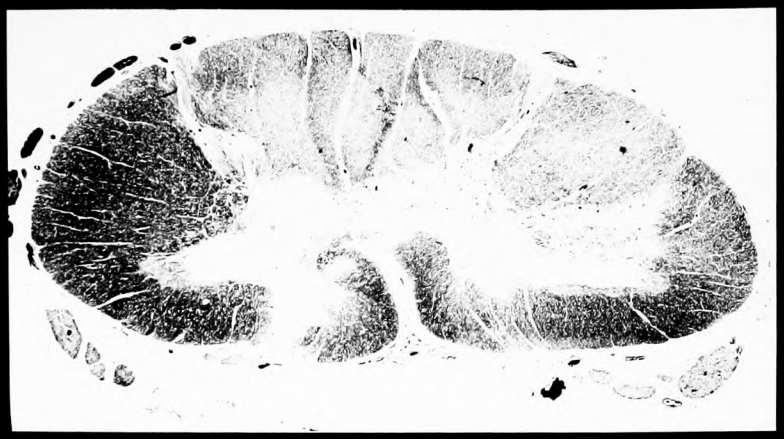
85

Figs. 86, 87, 88, 89.

These photomicrographs illustrate case 15. All are transverse sections of the spinal cord. (Figs. 86, 87, 89 Weil X 6·5, Fig. 88 Haematoxylin and Van Gieson X 6·6).

Fig. 86. C6.
Fig. 87. C7.
Fig. 88. C8.
Fig. 89. T1.

A large area of infarction affects the grey commissure, the anterior grey horns and parts of the white columns in C6, C7, and C8 sections. Lesser changes are present at T1.



86



87



88



89

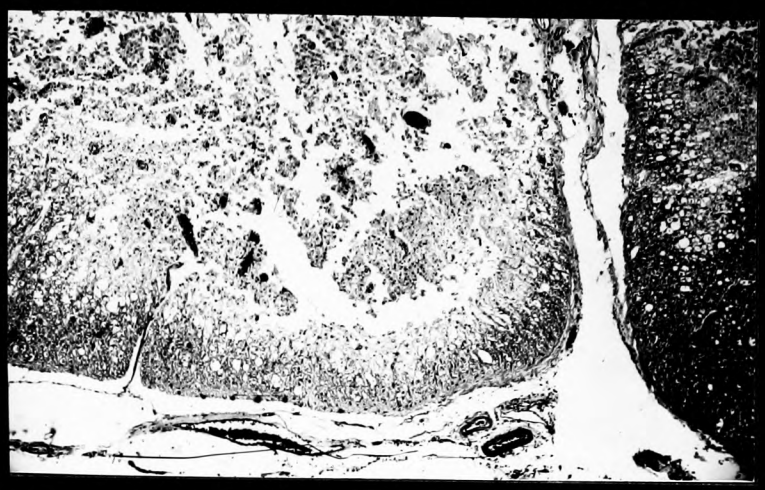
Figs. 90, 91, 92.

These photomicrographs illustrate case 15 and are all from transverse sections of the spinal cord.

Fig. 90. Anterior median sulcus and right anterior white column at C3 segmental level. Note the manner in which the area of infarction spares the peripheral rim of the white matter. (Haematoxylin and Van Gieson X 40).

Fig. 91. Anterior spinal artery and vein at C3 segmental level with ante-mortem thrombus blocking the anterior spinal artery. (Haematoxylin and eosin X 90).

Fig. 92. Anterior spinal vessels and anterior median sulcus at C4 segmental level. There is ante-mortem thrombus blocking a sulcal artery. (Haematoxylin and Van Gieson X 40).



90



91



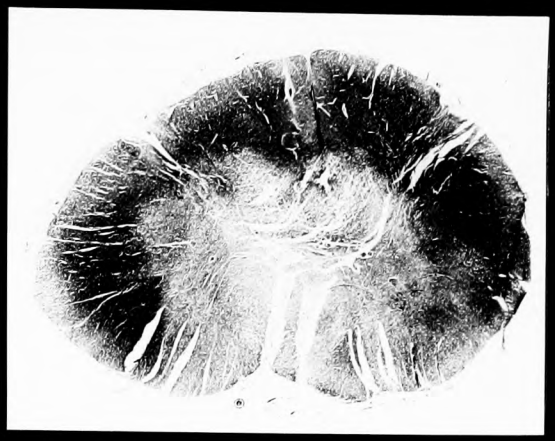
92

Figs. 93, 94, 95.

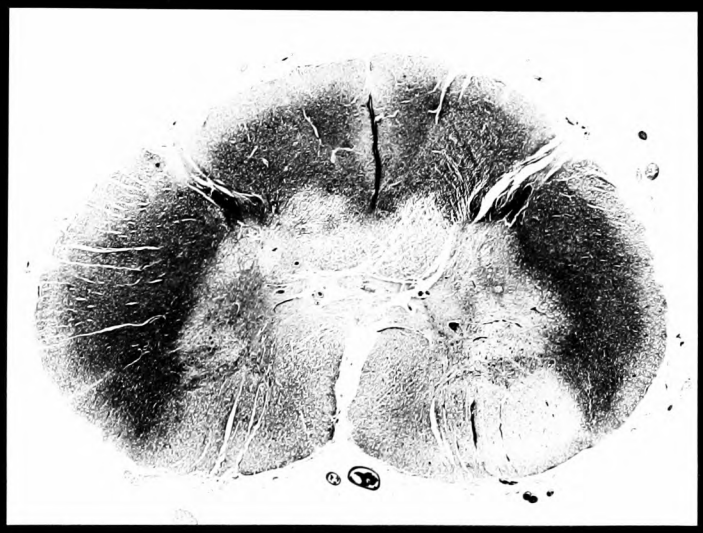
These photomicrographs illustrate case 16. They are all from transverse sections of the spinal cord stained for myelin. (Weil X 6·5).

Fig. 93. C4.
Fig. 94. C5.
Fig. 95. C6.

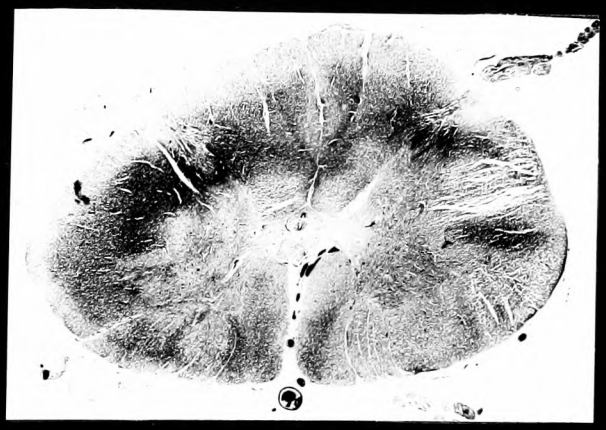
A continuous region of infarction extends through these three segments. The area is symmetrical and affects the grey commissure, the anterior grey horns and, the bases of the posterior horns. There is also infarction of most of the anterior white columns and those parts of the posterior and lateral white columns adjacent to grey matter.



93



94



95

Figs. 96, 97, 98.

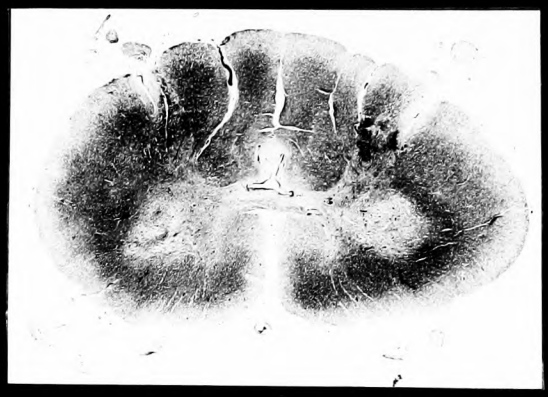
These photomicrographs illustrate case 16. They are all from transverse sections of the spinal cord stained for myelin. (Weil X 6·5).

Fig. 96. C7.
Fig. 97. C8.
Fig. 98. T1.

} The infarct seen in C4–6 (figs 93, 94, 95) extends throughout, C7, C8 and T1 spinal-cord segments and involves the grey commissure, the anterior horns, the bases of the posterior horns and some of the white matter adjacent to grey matter.



96



97



98

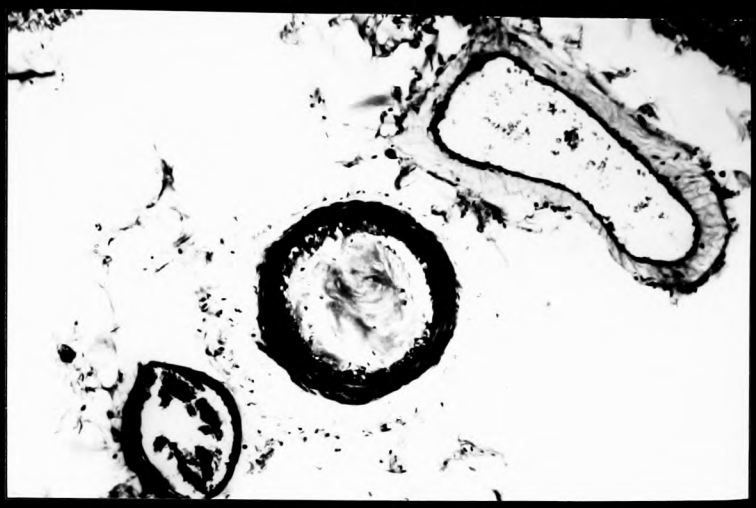
Figs. 99, 100, 101.

These photomicrographs illustrate case 16. They are all from transverse sections of the spinal cord.

Fig. 99. Anterior spinal artery and vein at C7 segmental level showing ante-mortem thrombus in the artery.
(Haematoxylin and Van Gieson X 45).

Fig. 100. Anterior spinal artery at C8 segmental level with ante-mortem thrombus in the lumen and extending into a sulcal artery branch.
(Haematoxylin and Van Gieson X 130).

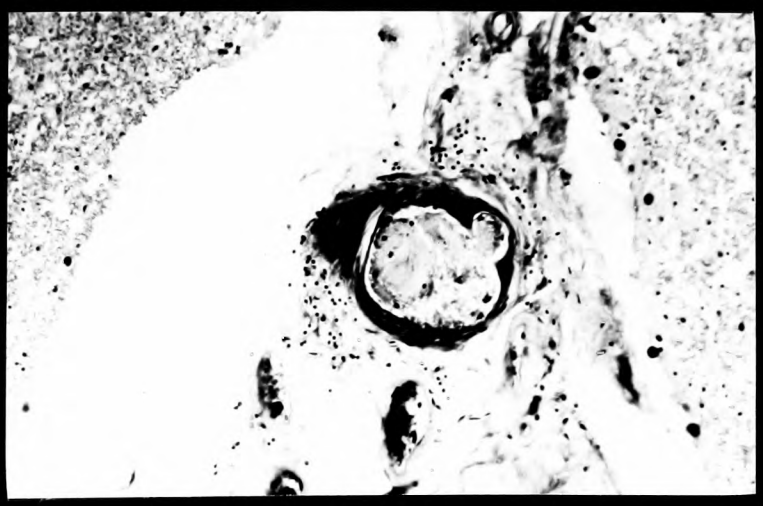
Fig. 101. Anterior median sulcus at C6 segmental level. There is ante-mortem thrombus blocking a sulcal artery.
(Haematoxylin and Van Gieson X 130).



99



100



101

Figs. 102, 103.

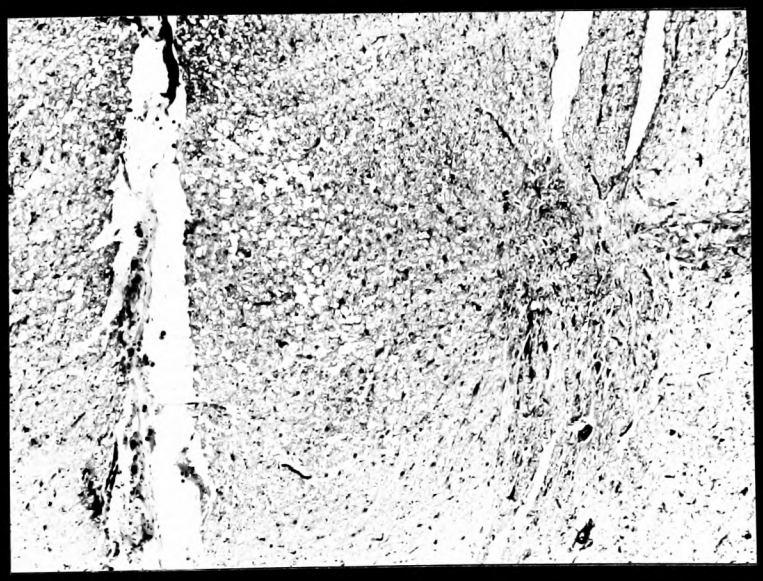
These photomicrographs illustrate case 16.

Fig. 102. Transverse section of spinal cord at C5 segmental level. The anterior horn shows changes of recent infarction. (Haematoxylin and eosin X 60).

Fig. 103. Anterior white column and anterior horn at C4 segmental level showing changes of recent infarction. (Haematoxylin and eosin X 45).



102



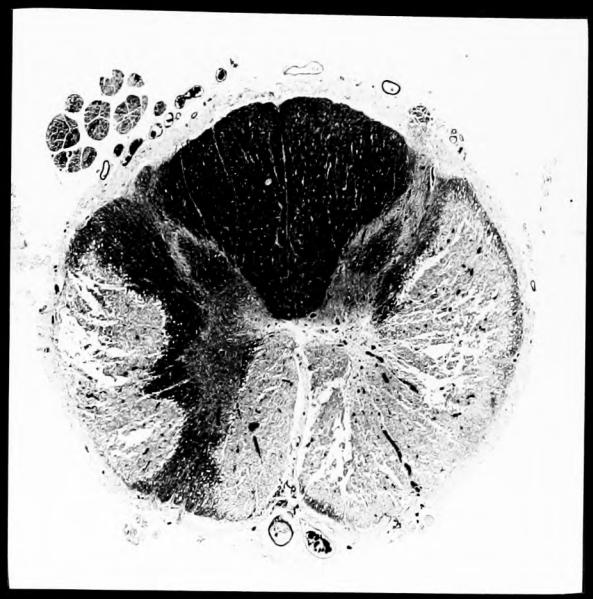
103

Figs. 104, 105.

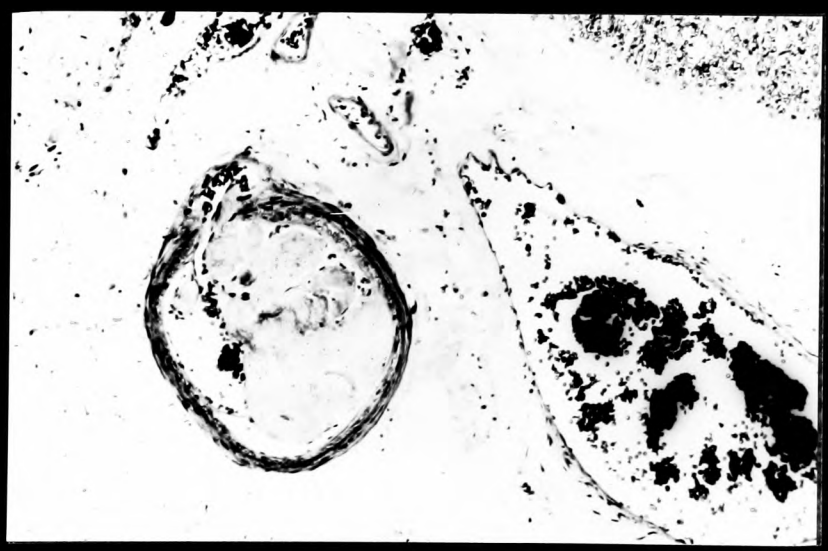
These photomicrographs illustrate case 17.

Fig. 104. Transverse sections of spinal cord at T11 segmental level. A large zone of infarction occupies an irregular and asymmetrical part of the cross-sectional area. (Weil X 8).

Fig. 105. Detail of anterior spinal artery and vein from same section as in fig 104. Ante-mortem thrombus blocks most of the lumen of the artery. (Weil X 130).



104



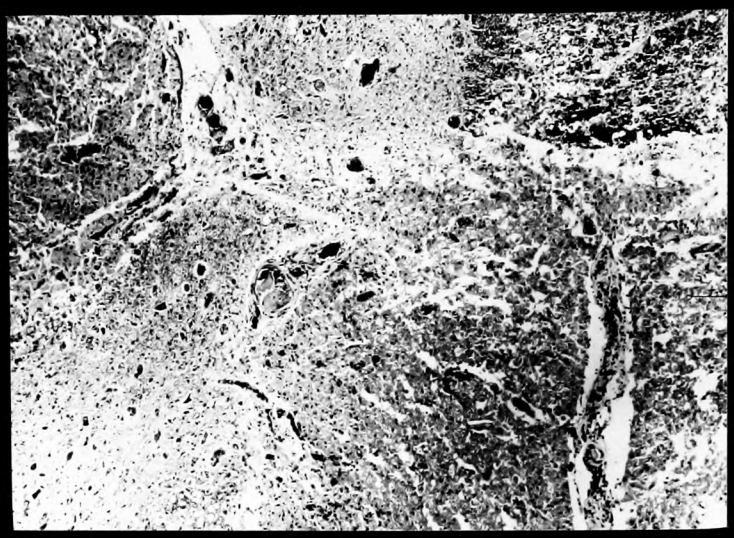
105

Figs. 106, 107.

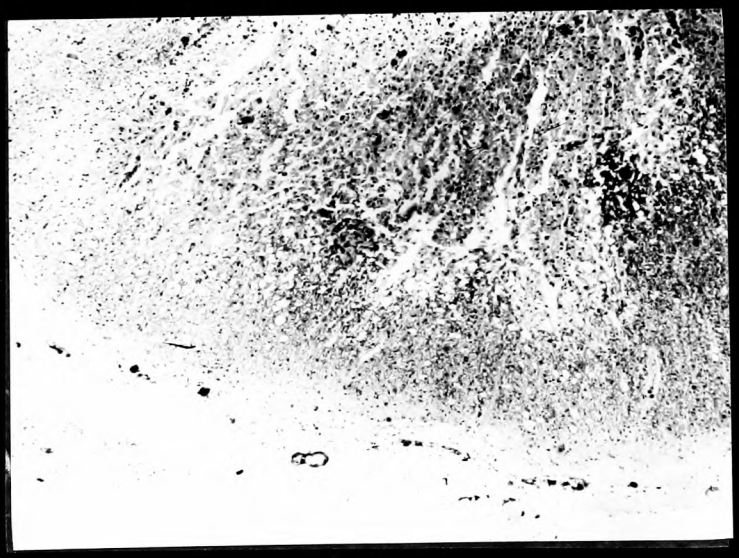
These photomicrographs illustrate case 17.

Fig. 106. Transverse section of spinal cord at L1 segmental level. The picture shows the infarcted area of the grey commissure, anterior horn and anterior white column. Ante-mortem thrombus is present in a sulco-commissural artery. (Haematoxylin and Van Gieson X 50).

Fig. 107. Transverse section of spinal cord at T11 segmental level. The picture shows the detail of the white matter infarction seen in fig 104. (Haematoxylin and Van Gieson X 50).



106



107

Figs. 108, 109, 110, 111.

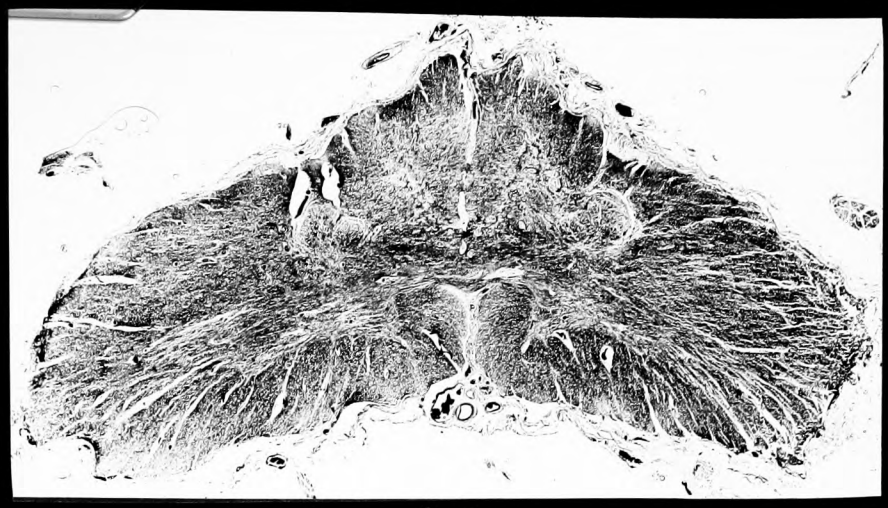
These photomicrographs illustrate case 18.

Fig. 108. Transverse section of the spinal cord at C6 segmental level where there is distortion due to cervical spondylosis. There is generalised atrophy of the grey and white matter. (Weil X 8).

Fig. 109. C7 segmental level. Detail of thickened leptomeninges. (Haematoxylin and Van Gieson x 130).

Fig. 110. C7 segmental level. Anterior median sulcus filled with connective tissue. (Haematoxylin and Van Gieson X 60).

Fig. 111. C2 segmental level. The grey commissure and adjacent areas are shown with connective tissue thickening of small intramedullary vessels. (Haematoxylin and Van Gieson X 60).



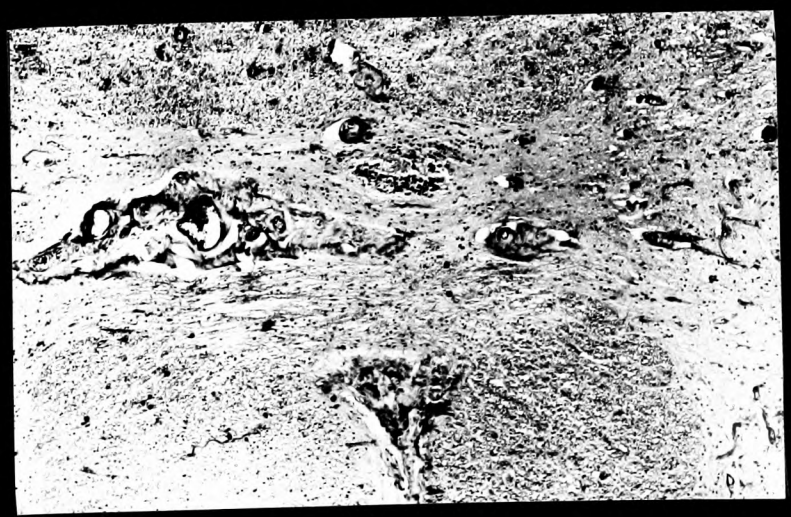
108



109



110



111

Figs. 112, 113, 114.

These photomicrographs illustrate case 18.

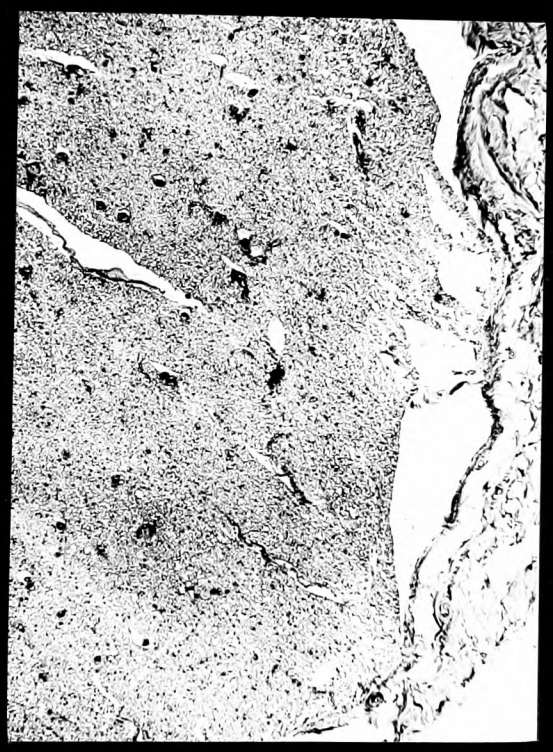
Fig. 112. C4 segmental level. The anterior spinal artery and vein are surrounded by acellular connective tissue. (Haematoxylin and Van Gieson X 60).

Fig. 113. C5 segmental level. The anterior white column shows gliosis and many capillaries surrounded by acellular connective tissue. (Haematoxylin and Van Gieson X 60).

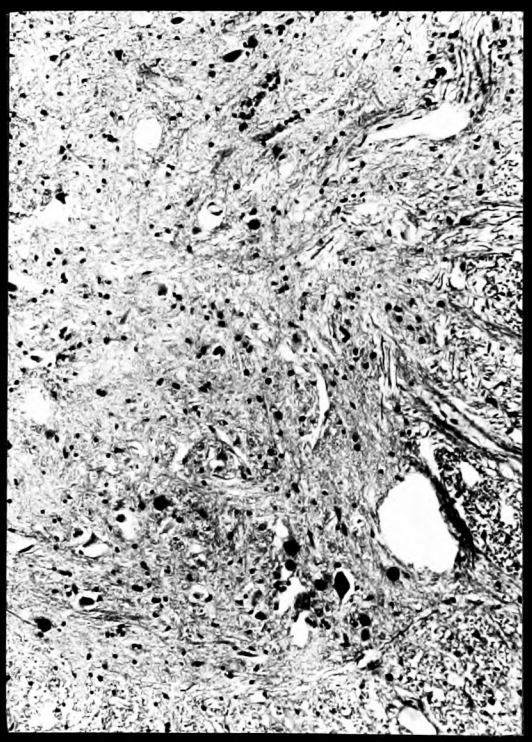
Fig. 114. C7 segmental level. The left anterior horn is shown. Very few neurone cell bodies remain. (Haematoxylin and eosin X 100).



112



113



114

Figs. 115, 116, 117.

These photomicrographs illustrate case 19. They are all of transverse sections of the spinal cord within the dura. (Haematoxylin and eosin X 5).

Fig. 115. C6.
Fig. 116. T4.
Fig. 117. T7.

The subarachnoid space is distended by tuberculous granulation tissue and the spinal cord shows severe ischaemic effects.



115



116



117

Figs. 118, 119, 120, 121.

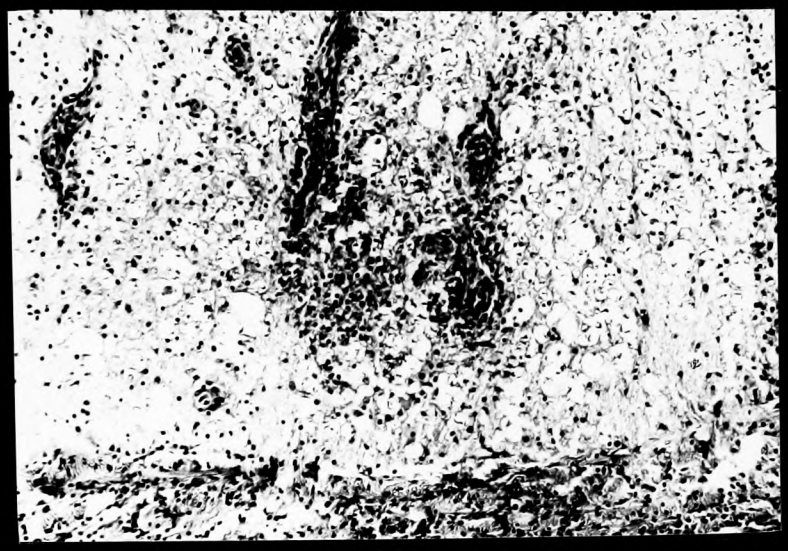
These photomicrographs illustrate case 19. They are all from transverse sections of the spinal cord.

Fig. 118. T7 segmental level. Detail of anterior white column to show endarteritis of short radial vessels. (Haematoxylin and eosin X 95).

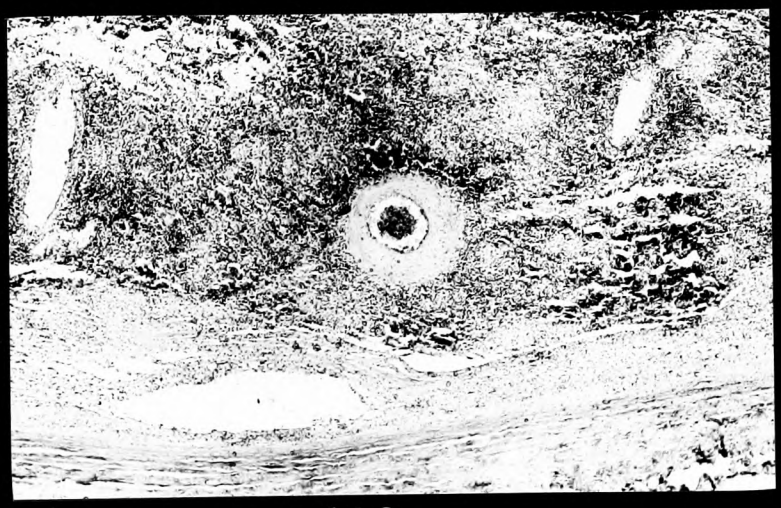
Fig. 119. T7 segmental level. Anterior spinal artery buried in exudate and showing concentric narrowing by endarteritis. (Haematoxylin and Van Gieson X 50).

Fig. 120. C6 segmental level. Endarteritis in a small coronal artery. (Haematoxylin and eosin X 425).

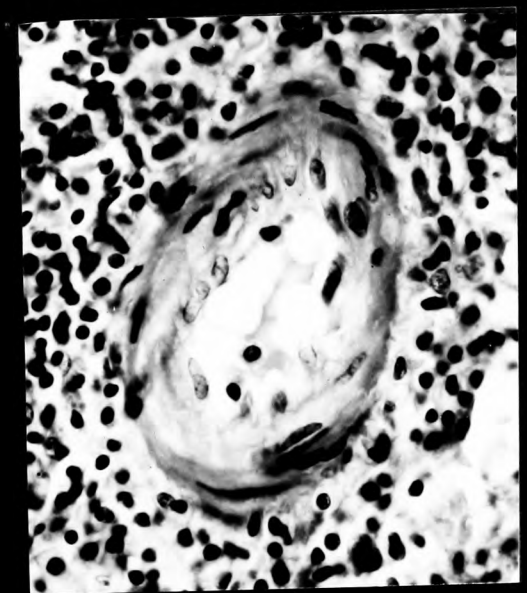
Fig. 121. T7 segmental level. Detail of endarteritis in anterior spinal artery. (Haematoxylin and eosin X 95).



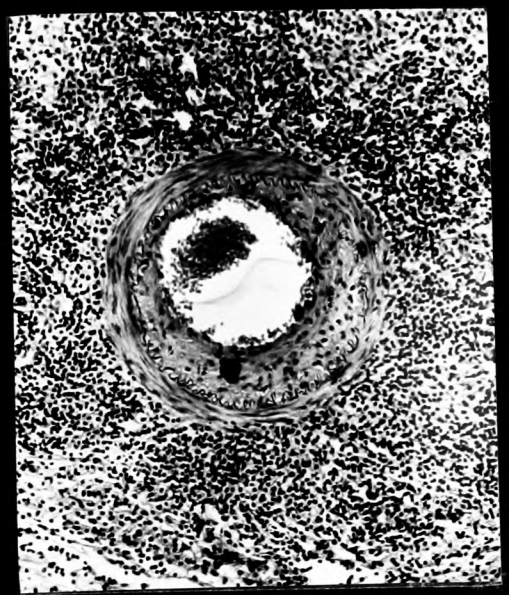
118



119



120



121

Figs. 122, 123, 124.

These photomicrographs illustrate case 20.

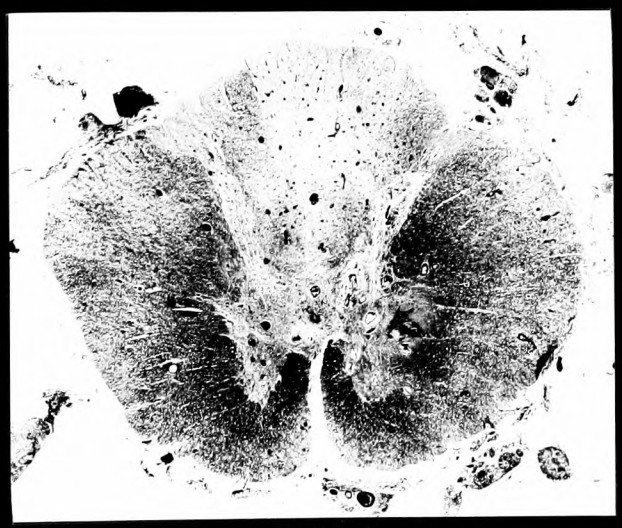
Fig. 122. Sarcoid granulation tissue in a sulcus near the insula. (Haematoxylin and Van Gieson X 50).

Fig. 123. Transverse section of spinal cord at T3 segmental level. There is sarcoid granulation tissue in relation to small vessels in the meninges and within the spinal cord. Wallerian degeneration is present in the posterior columns. (Weil X 8).

Fig. 124. Transverse section of spinal cord at T10 segmental level with similar findings to those seen in fig 123. (Weil X 6).



122



123



124

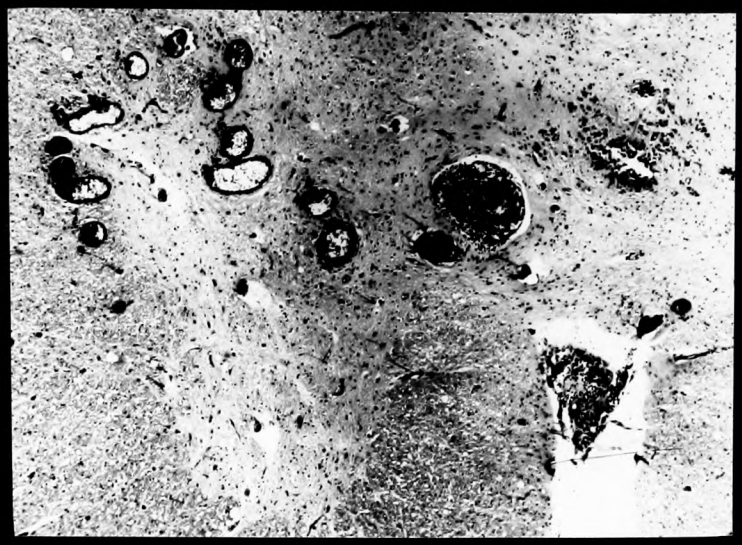
Figs. 125, 126, 127.

These photomicrographs illustrate case 20.

Fig. 125. T10 segmental level. Sarcoid granulation tissue is seen around a sulcal artery and around a sulco-commissural artery in the grey commissure. (Haematoxylin and Van Gieson X 50).

Fig. 126. L2 segmental level. The right anterior white column is shown where sarcoid granulation tissue is extending along the short radial blood vessels. (Haematoxylin and Van Gieson X 50).

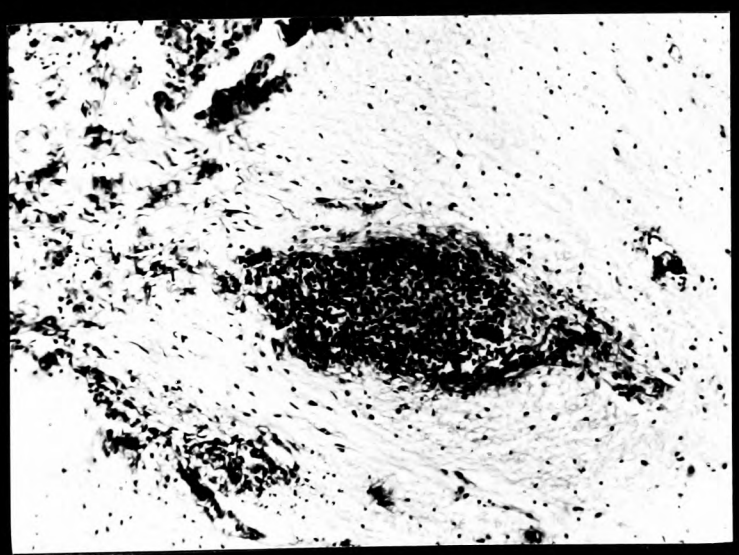
Fig. 127. T3 segmental level. The posterior root entry zone on the right side is shown. Granulation tissue is accompanying the long penetrating vessels. (Haematoxylin and Van Gieson X 120).



125



126



127

Figs. 128, 129.

These photographs illustrate case 21.

Fig. 128. Anterior aspect of lower thoracic and lumbar regions of the spinal cord. The anterior spinal artery is normal but the anterior spinal vein is enlarged and tortuous.

Fig. 129. Posterior aspect of lower thoracic and lumbar regions of the spinal cord. There is a large, tortuous vessel apparently additional to the normal venous system.



128



129

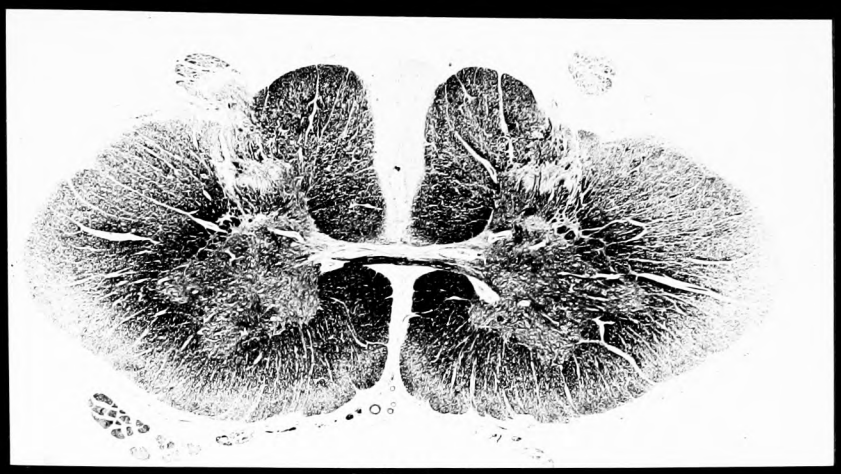
Figs. 130, 131, 132.

These photomicrographs illustrate case 21. They are all from transverse sections of the spinal cord stained for myelin. (Weil X 6·5).

Fig. 130. C7 segmental level. There is marked Wallerian degeneration in the posterior columns. The spinal vessels are normal at this level.

Fig. 131. T11 segmental level. The whole cross-sectional area of the spinal cord is necrotic. The anterior spinal vein is dilated and there is a large posterior vein.

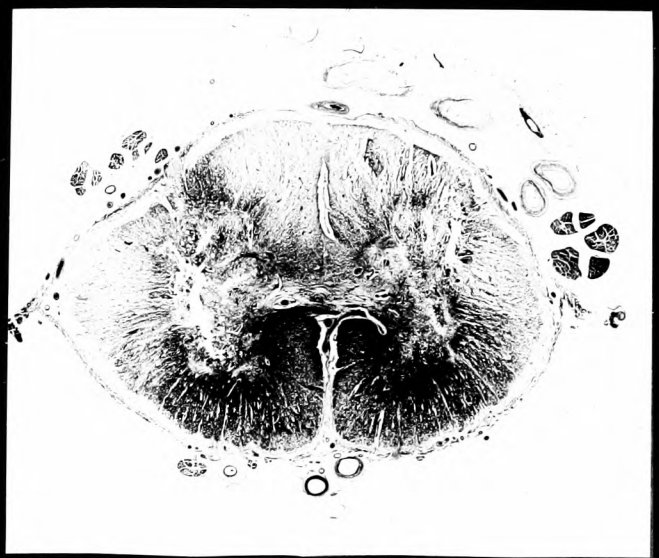
Fig. 132. L1 segmental level. There is partial necrosis at this level and some Wallerian degeneration evident in the pyramidal tracts. The anterior spinal vein is dilated and a large posterior vessel, an 'arterialised' vein, is cut several times because of its convoluted course.



130



131



132

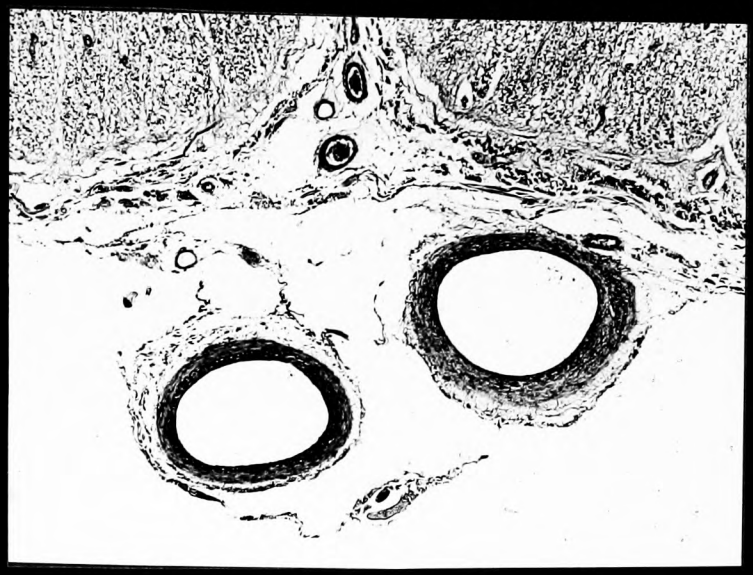
Figs. 133, 134, 135.

These photomicrographs illustrate case 21. They are all from transverse sections of the spinal cord at L1 segmental level.

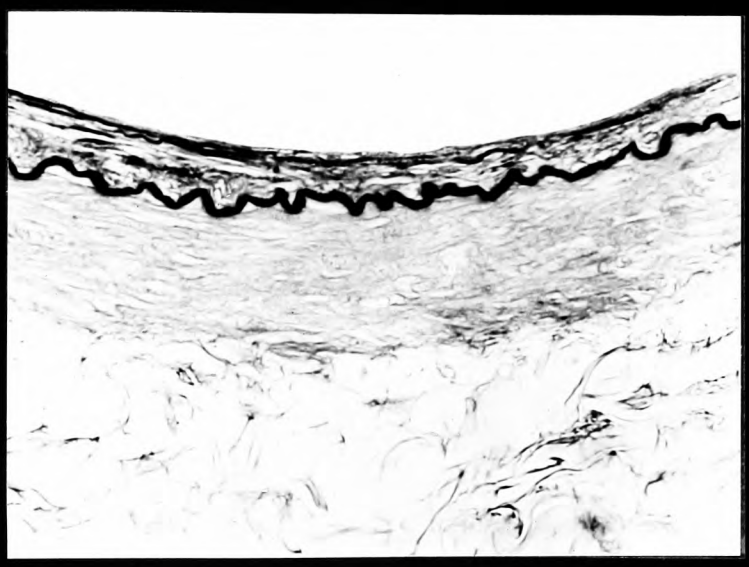
Fig. 133. Anterior spinal artery and vein. The vein (right) has a thickened wall. (Haematoxylin and eosin X 55).

Fig. 134. Wall of anterior spinal artery stained for elastic tissue. (Weigert's elastic stain X 450).

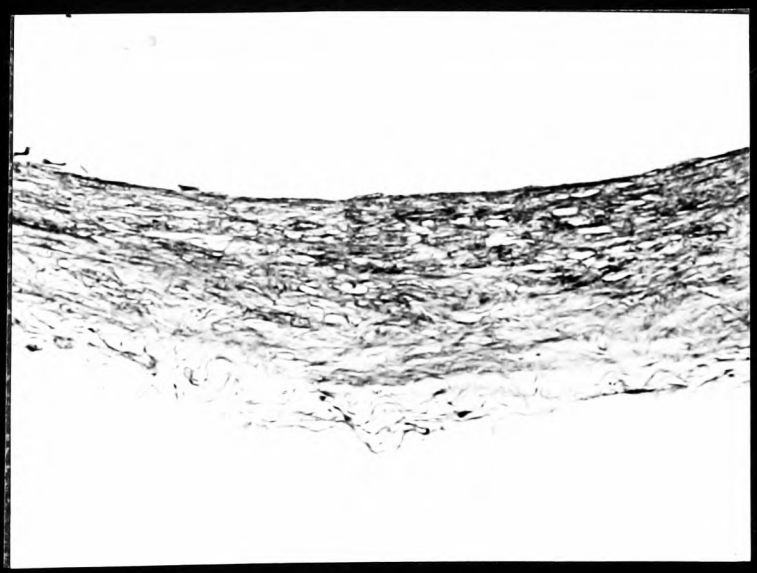
Fig. 135. Wall of anterior spinal vein stained for elastic tissue. (Weigert's elastic stain X 450).



133



134



135

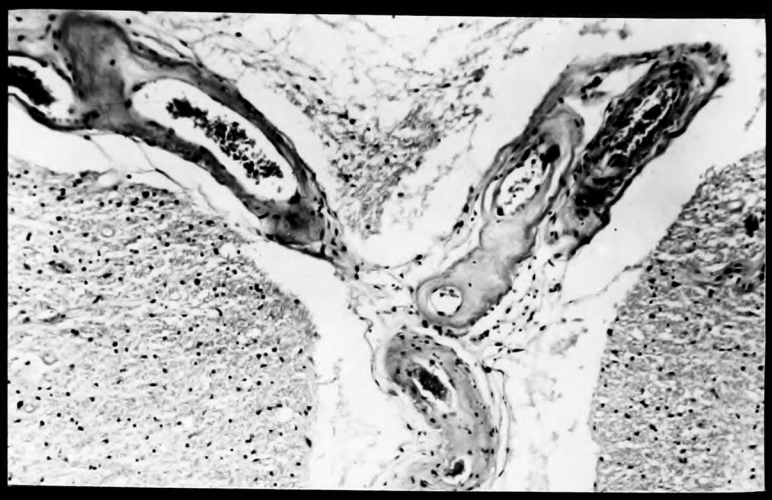
Figs. 136, 137, 138.

These photomicrographs illustrate case 21. They are all from transverse sections of the spinal cord at L1 segmental level.

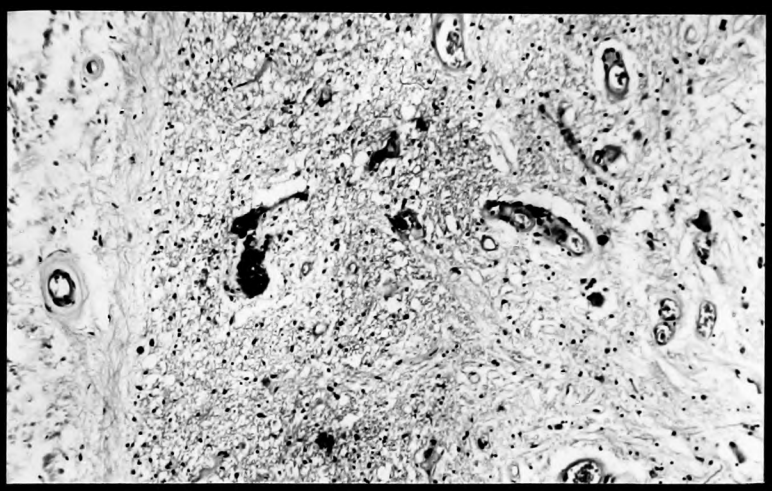
Fig. 136. Anterior median sulcus and grey commissure. A sulcal artery and vein are shown. Note that the wall of the vein is equal in thickness to that of the artery. (Haematoxylin and eosin X 90).

Fig. 137. Anterior white column showing dilated short radial veins with hyaline thickening of their walls. Haemosiderin pigment is present in the perivascular spaces.
Haematoxylin and eosin X 90).

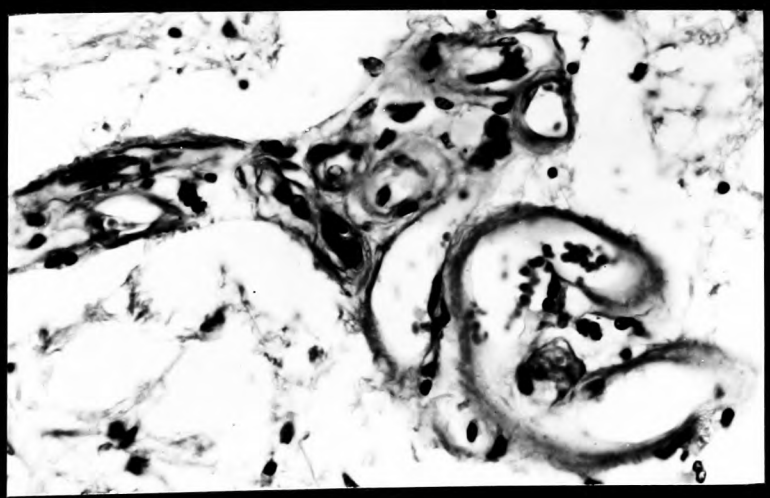
Fig. 138. Enlarged view of abnormal intramedullary vessels.
(Haematoxylin and eosin X 450).



136



137



138

Figs. 139, 140.

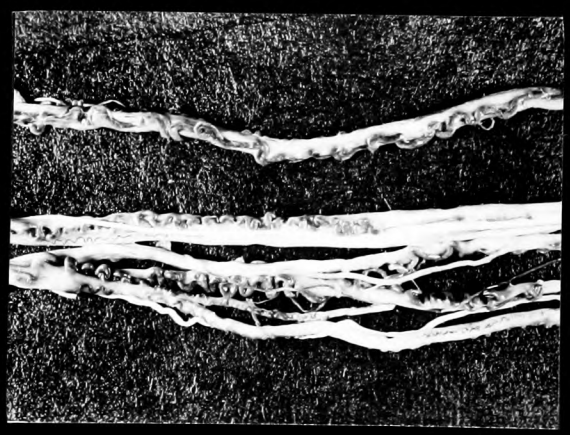
These photographs illustrate case 22.

Fig. 139. Posterior aspect of spinal cord showing enormously distended and convoluted posterior vessel. The roots of the cauda equina have large accompanying vessels. (Life size).

Fig. 140. Detail of roots of cauda equina (X 2).



139



140

Figs. 141, 142, 143, 144.

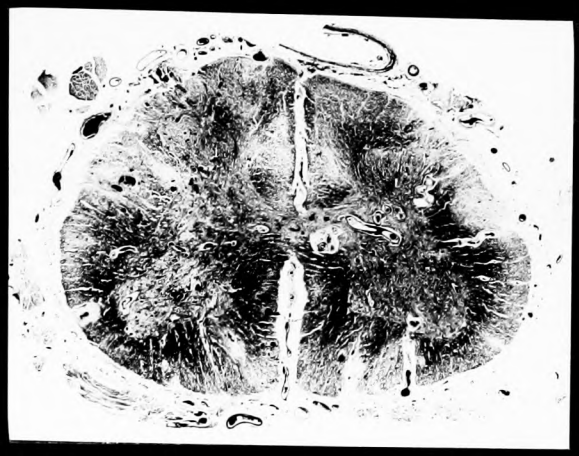
These photomicrographs illustrate case 22. They are all from transverse sections of the spinal cord.

Fig. 141. L2 segmental level
Fig. 142. S1 segmental level

} There is partial necrosis of the spinal cord. The anterior spinal vein is enlarged and there is a large convoluted posterior vessel. (Weil X 6·5).

Fig. 143. Left grey column at L2 segmental level showing abnormal intramedullary vessels. (Haematoxylin and eosin X 45).

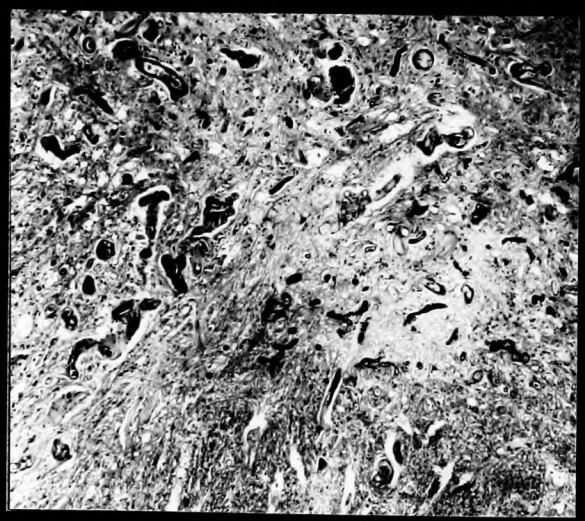
Fig. 144. Anterior spinal vessels at S1 segmental level. Note the grossly enlarged anterior spinal vein which has an "arterialised" wall. (Haematoxylin and eosin X 45).



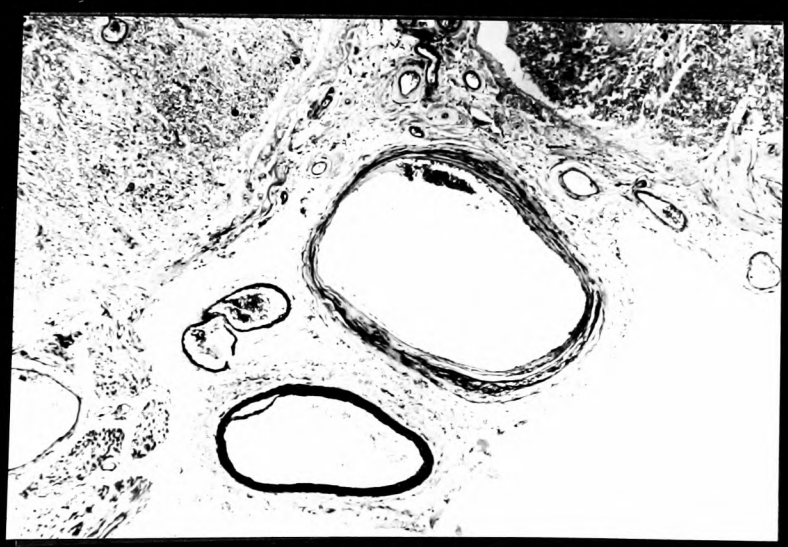
141



142



143



144

Figs. 145, 146, 147, 148.

These photomicrographs illustrate case 23. They are all from transverse sections of the spinal cord.

Fig. 145. C5 segmental level. There is marked Wallerian degeneration in the posterior columns. (Weil X 7·5).

Fig. 146. L2 segmental level. Abnormal intramedullary vessels near the central canal. (Haematoxylin and Van Gieson X 140).

Fig. 147. T10 segmental level. This myelin stained transverse section shows severe necrosis of grey and white matter. The anterior spinal vein is enlarged and there is a large vein, cut several times, on the posterior aspect of the spinal cord (Weil X 7·5).

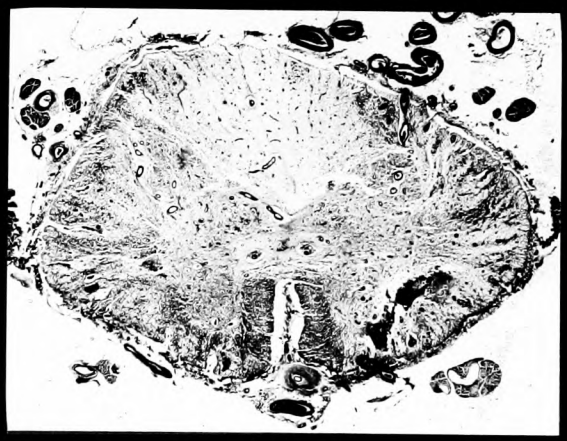
Fig. 148. Detail of anterior spinal vessels at T10 segmental level. The anterior spinal veins appear to have been thrombosed and recanalised. (Haematoxylin and eosin X 55).



145



146



147



148

Figs. 149, 150, 151, 152.

These photomicrographs illustrate case 24. They are all from transverse sections of the spinal cord stained for myelin. (Weil X 8).

Fig. 149. C4 segmental level. There is Wallerian degeneration seen in the posterior columns.

Fig. 150. T5 segmental level. In addition to Wallerian degeneration as in C4, there are moderately dilated intramedullary vessels and there is a large anterior spinal vein.

Fig. 151. L1 segmental level. There is widespread necrosis in addition to Wallerian degeneration in the posterior columns. All the spinal veins are greatly enlarged. A large posterior vessel is cut several times because of its convolution.

Fig. 152. L5 segmental level. To the changes in L1 are added severe necrosis with central cavitation of the spinal cord.



149



150



151



152

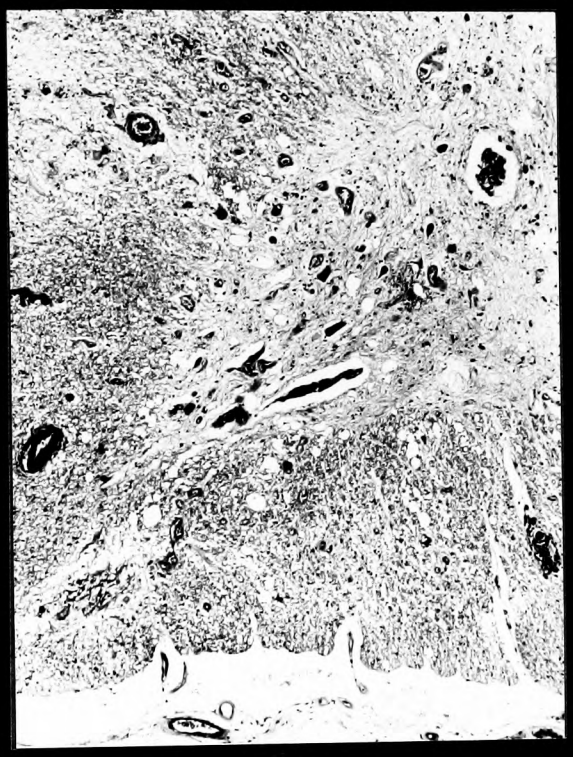
Figs. 153, 154, 155.

These photomicrographs illustrate case 24. They are all from transverse sections of the spinal cord.

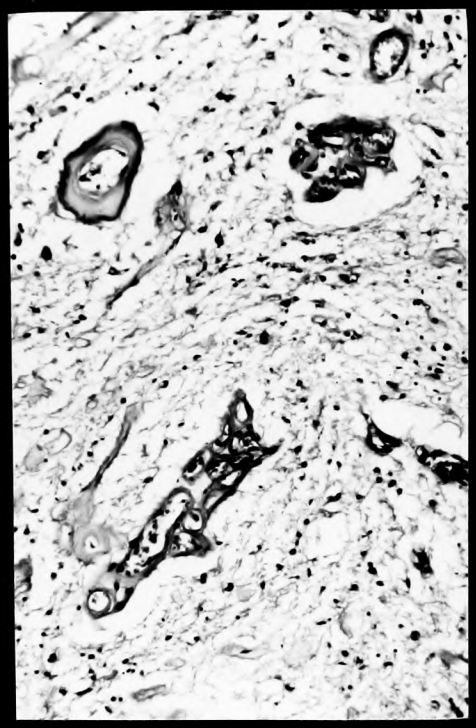
Fig. 153. Anterior horn at L1 segmental level showing abnormal intramedullary vessels. (Haematoxylin and eosin X 50).

Fig. 154. Detail of abnormal vessels at L5 segmental level. (Haematoxylin and eosin X 120).

Fig. 155. S2 segmental level. The vessel shown is an "arterialised" vein on the posterior aspect of the spinal cord. (Haematoxylin and eosin X 50).



153



154



155

Figs. 156, 157, 158.

These photomicrographs illustrate case 25. They are all from transverse sections of the spinal cord.

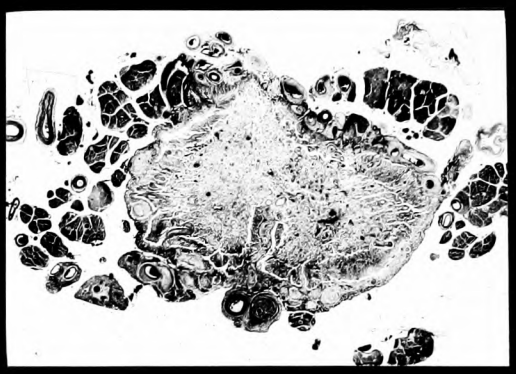
Fig. 156. L1 segmental level. The white matter has undergone partial necrosis. The anterior spinal vein is hypertrophied and there is a large abnormal vessel on the posterior aspect of the spinal cord. (Weil X 8).

Fig. 157. S3 segmental level. The spinal cord is almost completely destroyed with very little grey or white matter remaining. There are abnormal intramedullary vessels and enlarged spinal veins. A large abnormal posterior vessel is present. (Weil X 8).

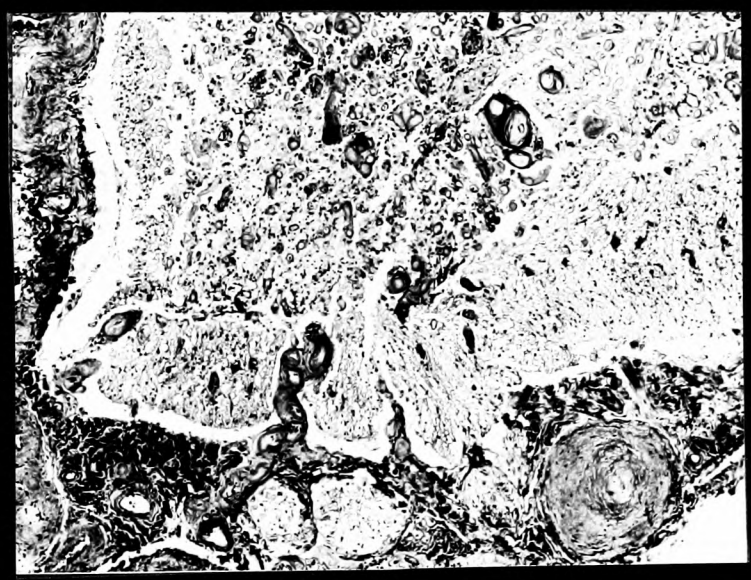
Fig. 158. Detail of left anterior white column at S3 segmental level. (Haematoxylin and Van Gieson X 50).



156



157



158